

Atomic processes relevant for high-temperature plasmas

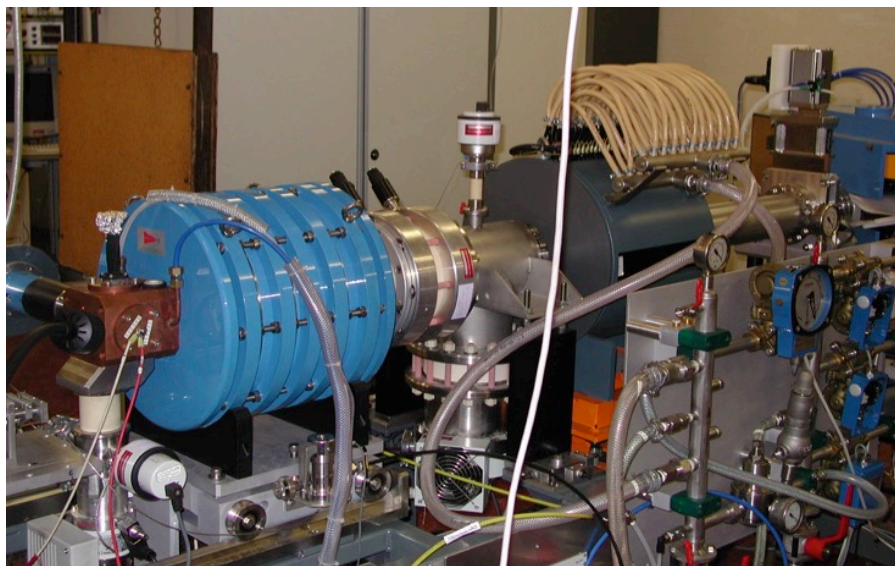
Pedro Amaro

Laboratório de Instrumentação, Engenharia Biomédica e Física da Radiação (LIBPhys-UNL), Departamento de Física, Faculdade de Ciências e Tecnologia, FCT, Universidade Nova de Lisboa, 2829-516 Caparica, Portugal

Outline of the talk

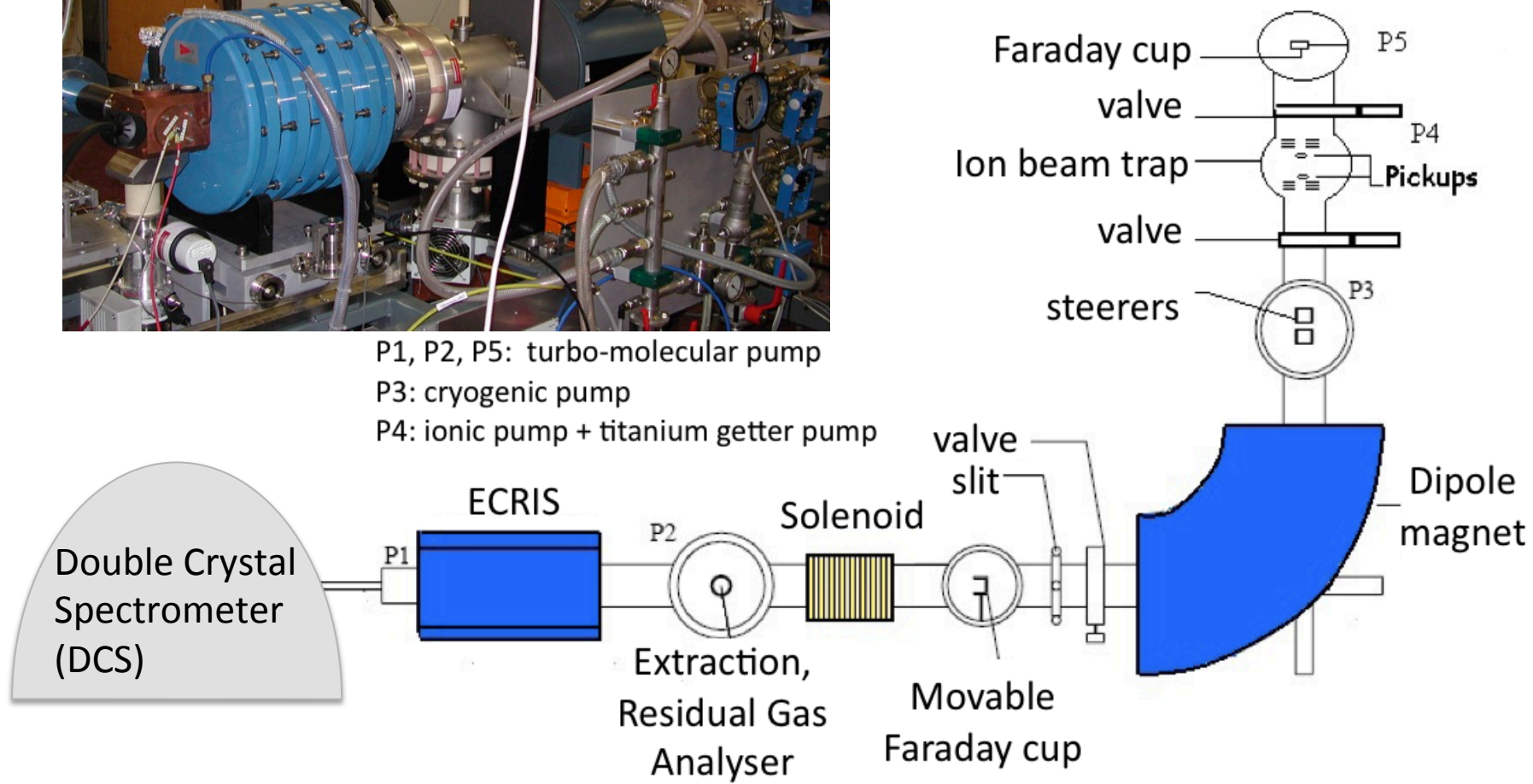
- High-precision reference-free measurements of x-ray transitions in ECRIS plasma
 - Probe and provide tests of BSQED and relativistic effects
 - x-ray standards.
- X-ray spectroscopy in EBIT plasma
 - Iron x-ray lines of astrophysical interest
 - Accurate measurement of electron collision cross sections
 - Preliminary measurements in tungsten
- Electron impact ionization cross section expression
 - Relativistic Binary Encounter Dipole model
 - Calculations for highly charged Kr and U

The SIMPA ECR Ion Source Laboratory



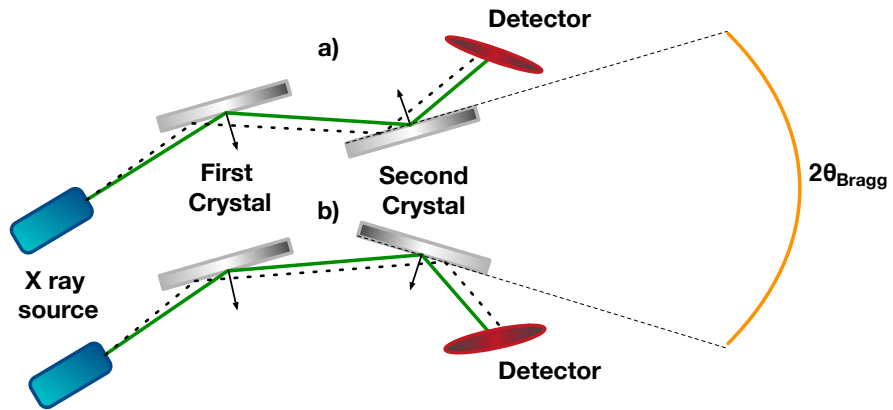
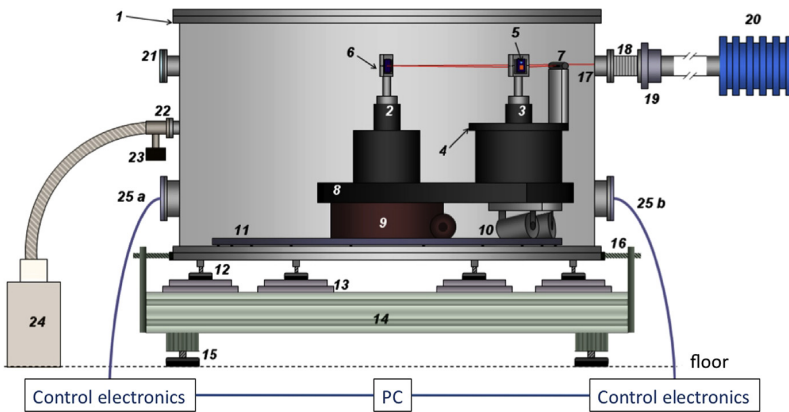
I N S P
Institut des NanoSciences de Paris

LKB



Double crystal spectrometer

The Bragg condition: $n\lambda=2d \sin(\theta_B)$
can be satisfied in two orientations of the second crystal



The angle difference between the two peak positions is directly correlated to the Bragg angle of the transition in question according to

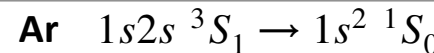
$$\theta_B = [180 - (\theta_{disp} - \theta_{nondis})]/2$$

High-accurate reference-free measurements

DCS simulations

Method:

P. Amaro, et. al, Phys. Rev. Lett. 109, 043005(2012).

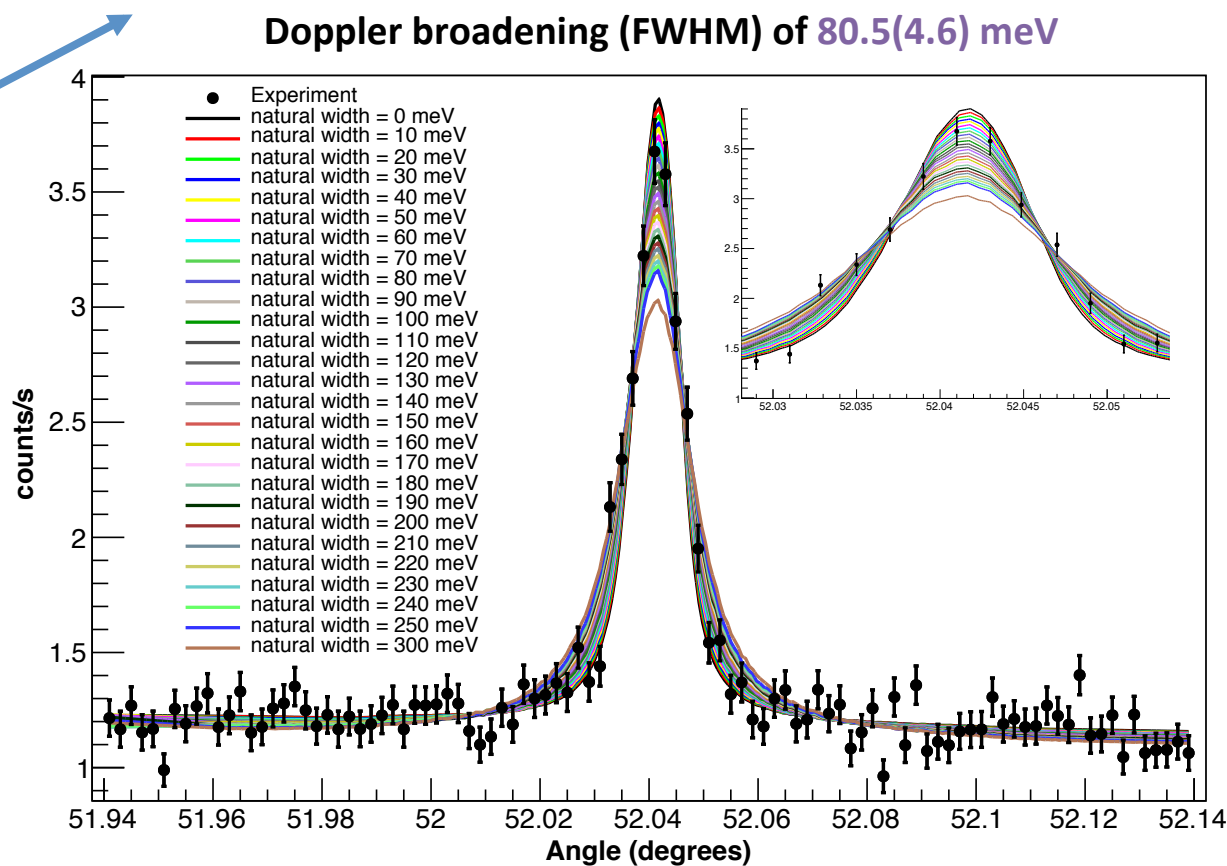


Natural Width < 10^{-6} eV

- Perform several simulations with the calculated theoretical energy (E_{th}) and different Lorentzian width (Γ_L);
- Exp. Gaussian Broadening (Γ_G);
- Interpolate the simulated output spectra with splines;
- Fit the antiparallel spectra with the parametrized interpolated functions

$$I(\theta - \theta_0) = I_{max} S(\theta - \theta_0) + a + b\theta$$

- Get the χ^2 for each performed fit with the optimized fit coefficients by the the χ^2 minimization.



P. Amaro, et. al, Radia. Phys.s and Chems 98, 132 (2014).

Latest Measured transitions

- 4 x-ray transitions have been measured in 3 different argon charged states:

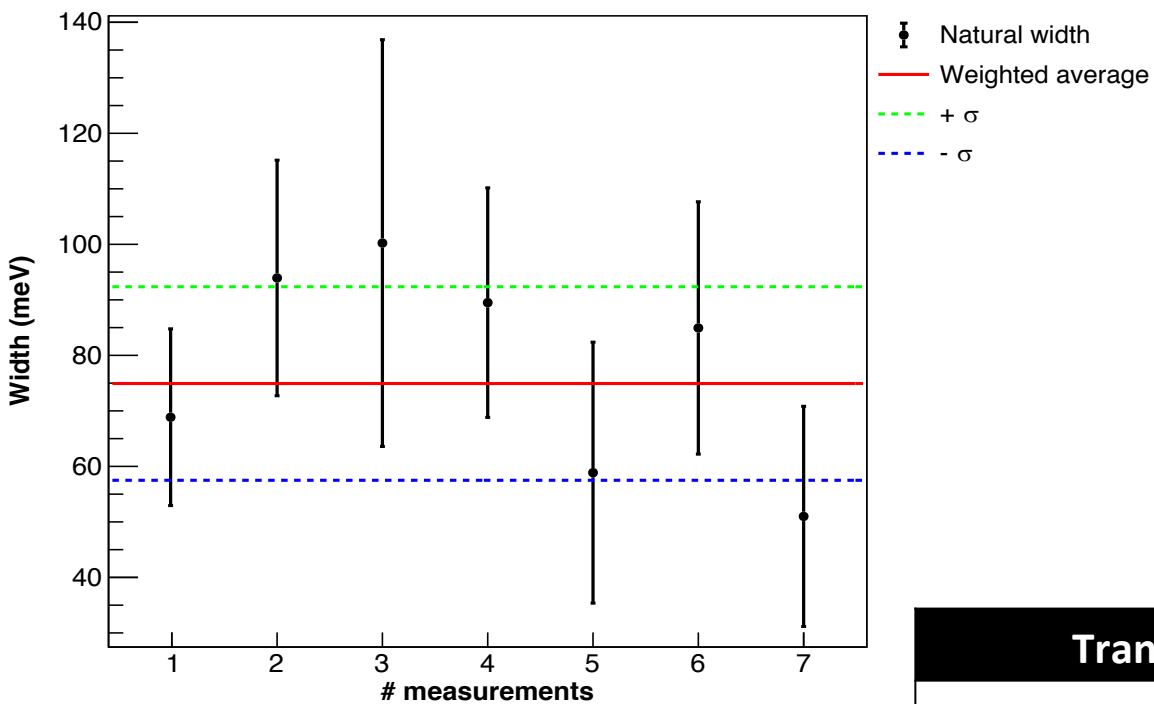
He-like Ar: $1s\ 2p\ ^1P_1 \rightarrow 1s^2\ ^1S_0$

Be-like Ar: $1s\ 2s^2\ 2p\ ^1P_1 \rightarrow 1s^2\ 2s^2\ ^1S_0$

J. Machado, et. al, Phys. Rev. A 97, 032517 (2018)

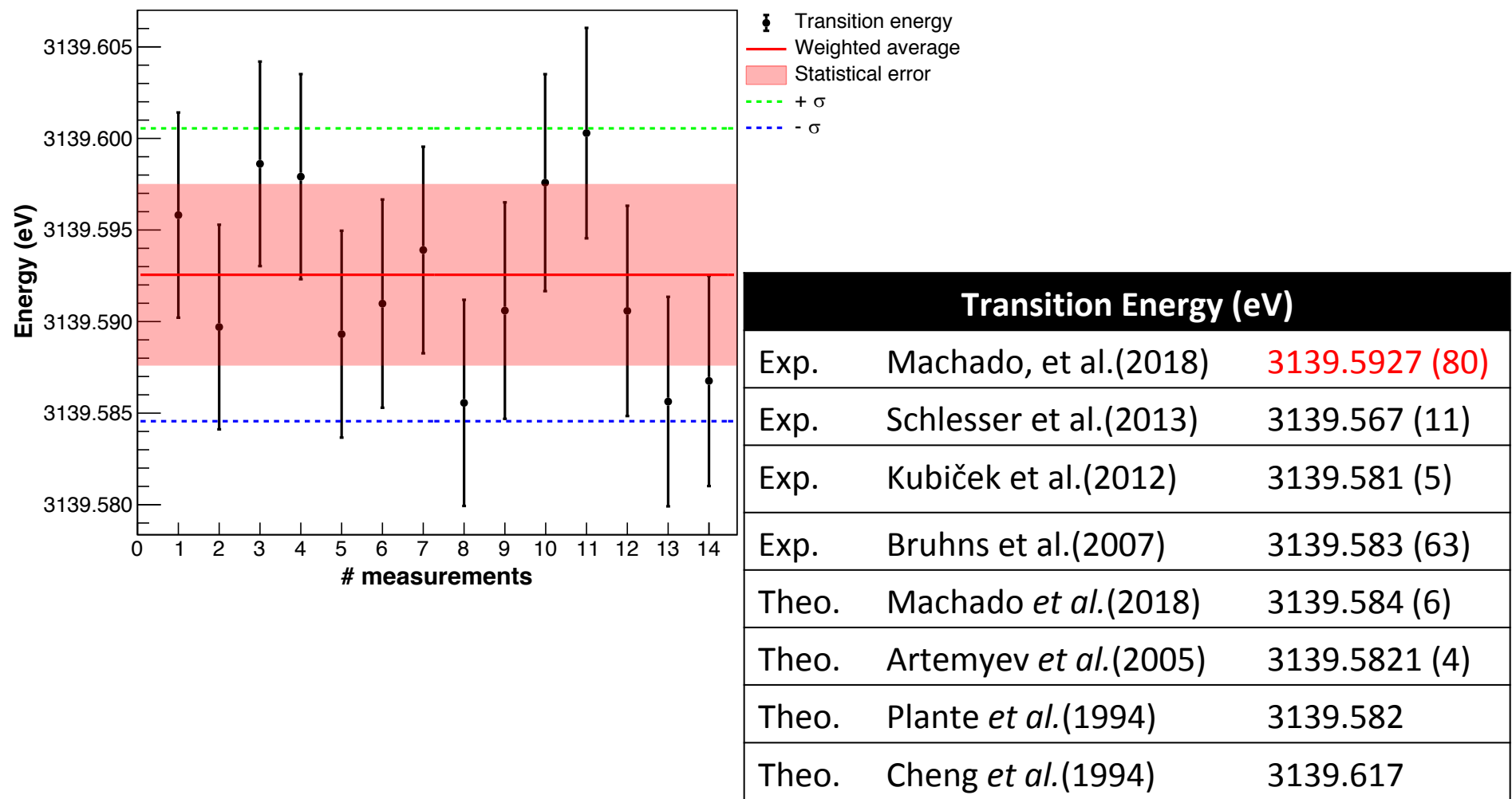
Li-like Ar: $1s\ 2s\ 2p\ ^2P_J \rightarrow 1s^2\ 2s\ ^2S_{1/2}, J = 1/2, 3/2$

$1s\ 2p\ 1P_1 \rightarrow 1s2\ 1S_0$ transition in He-like Ar



Transition Natural Width (meV)		
Exp.	Machado, et al.(2018)	75 (17)
Theo.	Johnson et al.(1995)	70.43
Theo.	Machado et al.(2018)	70.4778 (25)
Theo.	Drake (1979)	70.49 (14)

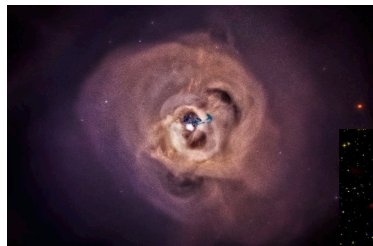
$1s\ 2p\ 1P_1 \rightarrow 1s2\ 1S_0$ transition in He-like Ar



Summary of the goals

- ✓ Presented a high accurate spectrometer
 - ✓ Accuracies up to few ppm@keV
 - ✓ Reference-free
- ✓ Provide high-accurate energy and widths
 - ✓ He-like, Be-like and Li-like Ar
 - ✓ Data for S is currently being analyzed
- ✓ Can be highly profitable in spectra diagnostics based on special x-ray lines, specially metastable ones

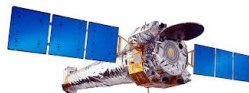
X-ray spectroscopy in astrophysics



Perseus galaxy cluster

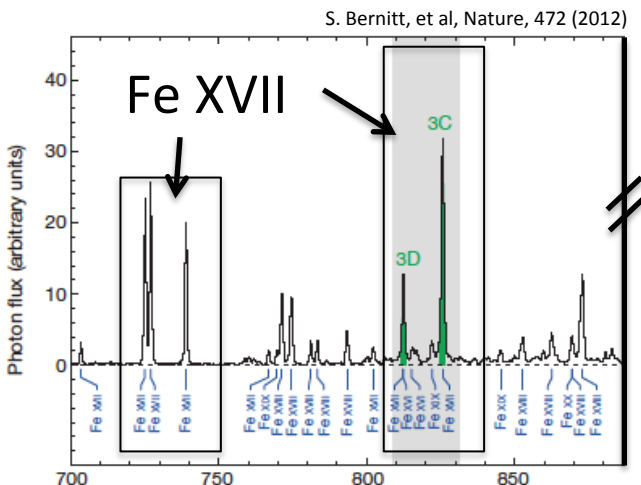


Cassiopeia A



NASA CHANDRA

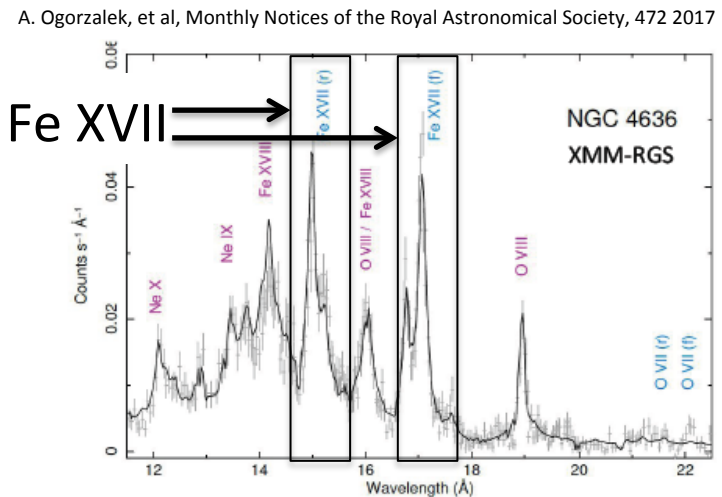
HETG High Energy Transmission Grating Spectrometer (0.4-10 keV) ~1 eV@1 keV



ESA XMM-Newton
RGS - Reflection Grating
Spectrometer (0.35-2.5 keV)
~2 eV@1keV



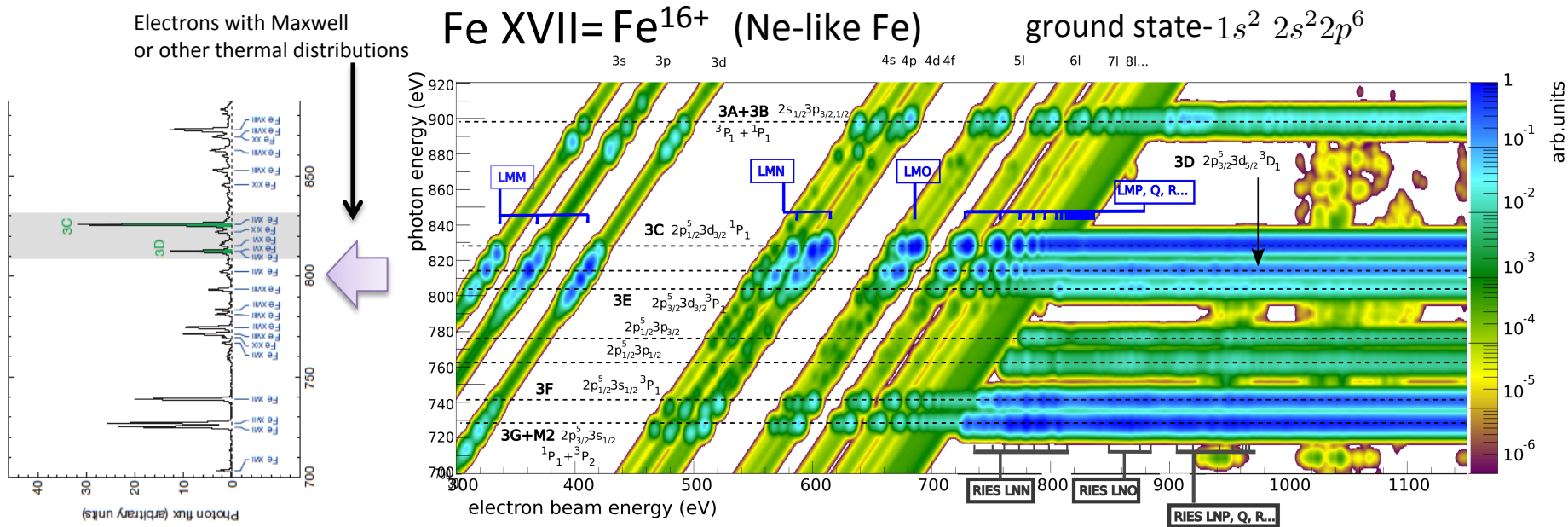
JAXA ASTRO-H/Hitomi/XARM
SXS micro-calorimeter (0.3-10 keV)
~5 eV@6keV



- Interpretation relies heavily on atomic data and plasma modeling and provides diagnostics of:
 - Ionic and electron temperatures
 - Densities and elemental abundances
 - X-ray opacities and velocity turbulences
 - Well-known codes: SPEX and AtomDB

de Plaa, A&A, 539, 2012 and refs thererin

XVII Fe L-shell data

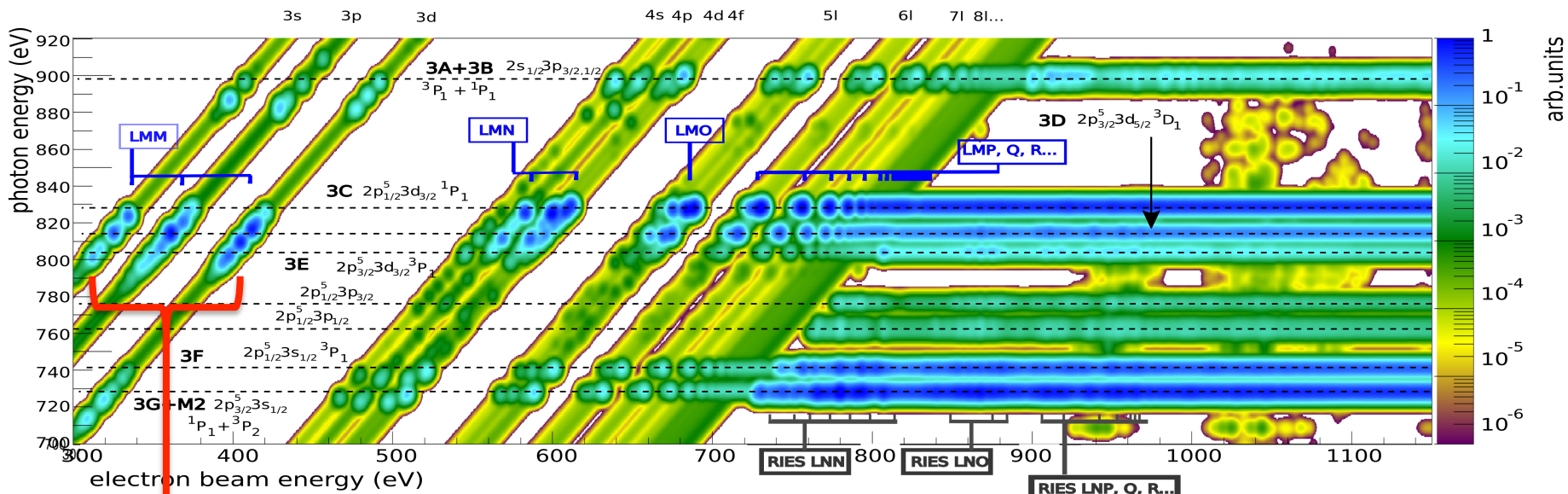


Important lines for x-ray opacity diagnostics based on photon resonant scattering

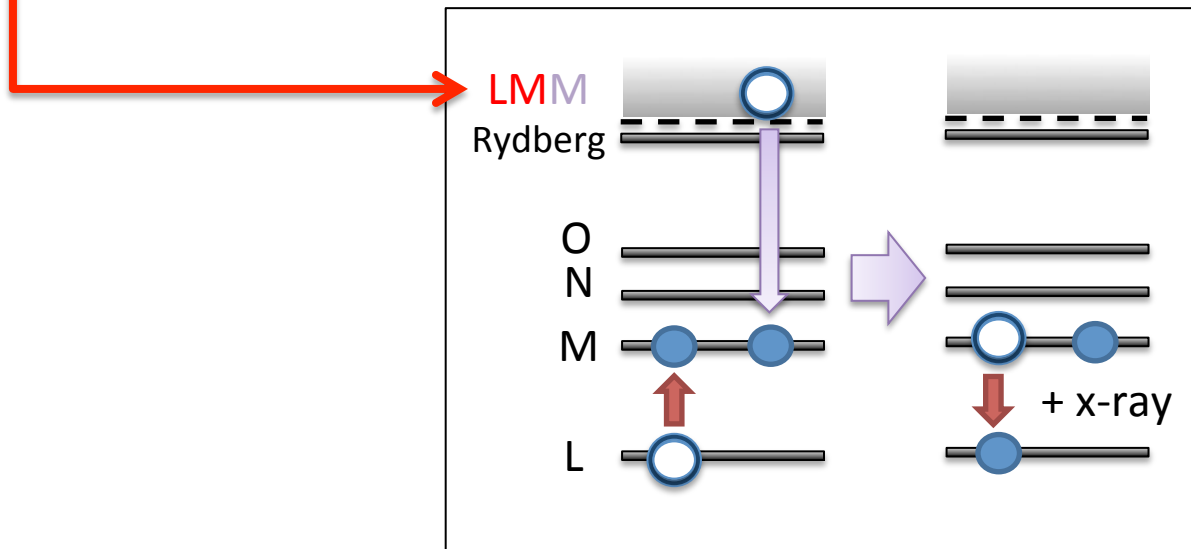
- **3C** $2p_{1/2}^5 3d_{3/2} \ ^1P_1$
- **3D** $2p_{3/2}^5 3d_{5/2} \ ^3D_1$
- **3C/3D ratio**
 - Low cascade contributions
 - R. Mewe et al, A&A, 368, 888-900 (2001).
 - 3C collision strengths inconsistent with predictions
 - e.g. G. V. Brown, et al PRL, 96, 253201 (2006)
 - e.g. S. Bernitt, et al, Nature, 472, 225 (2012)
- **3F** $2p_{1/2}^5 3s_{1/2} \ ^3P_1$
- **3G+M2** $2p_{3/2}^5 3s_{1/2} \ ^1P_1 + ^3P_2$
- **3F/(3G+M2) ratio**
 - M2 is optically thinner (M2 transition)
 - J. de Plaa, et al A&A, 539 (2012).
 - Complex cascade contributions
 - No experimental data available
 - Residual theoretical predictions



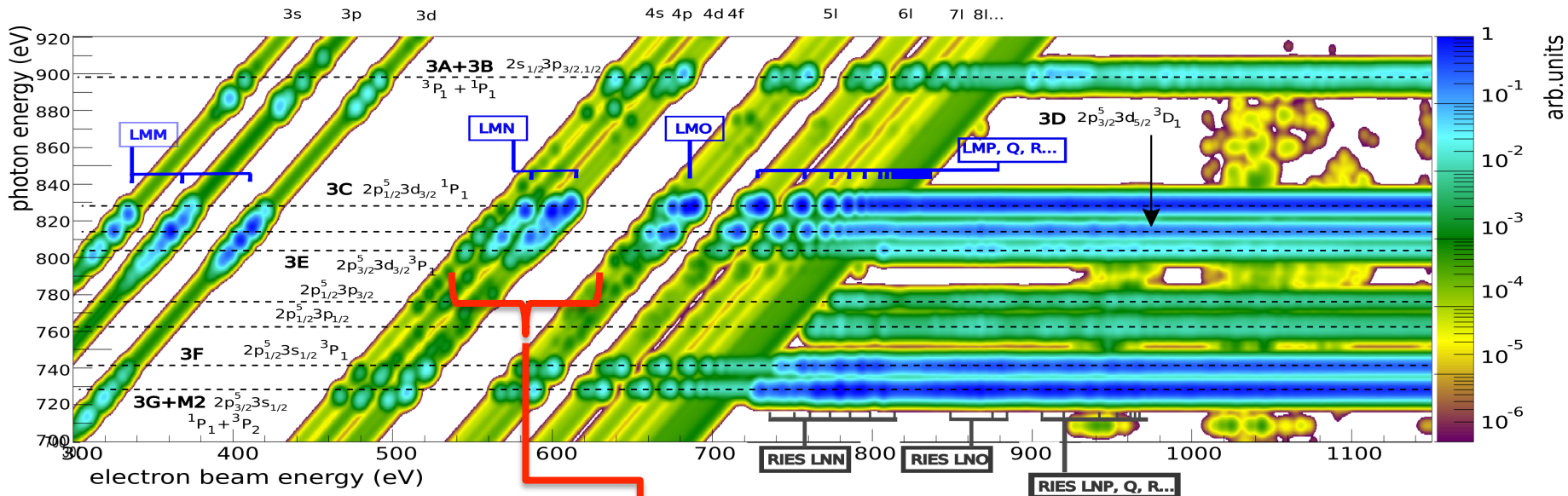
Atomic processes in Fe XVII



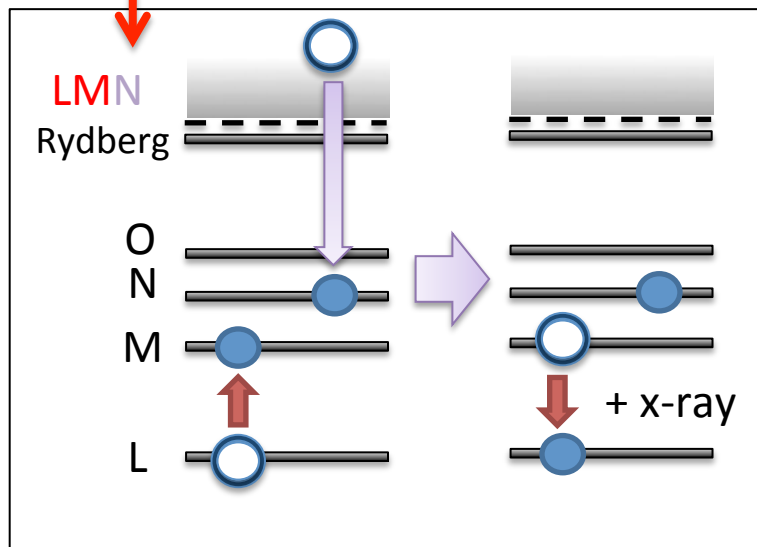
Dielectronic recombination (DR)



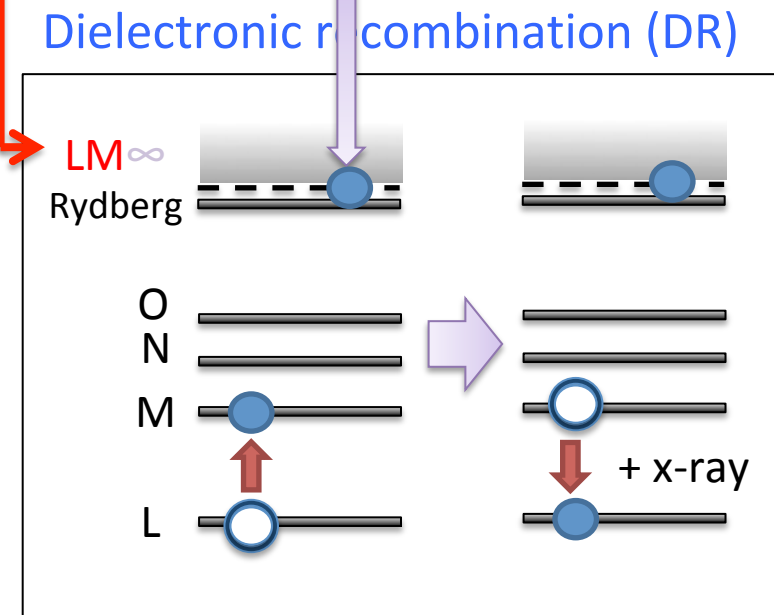
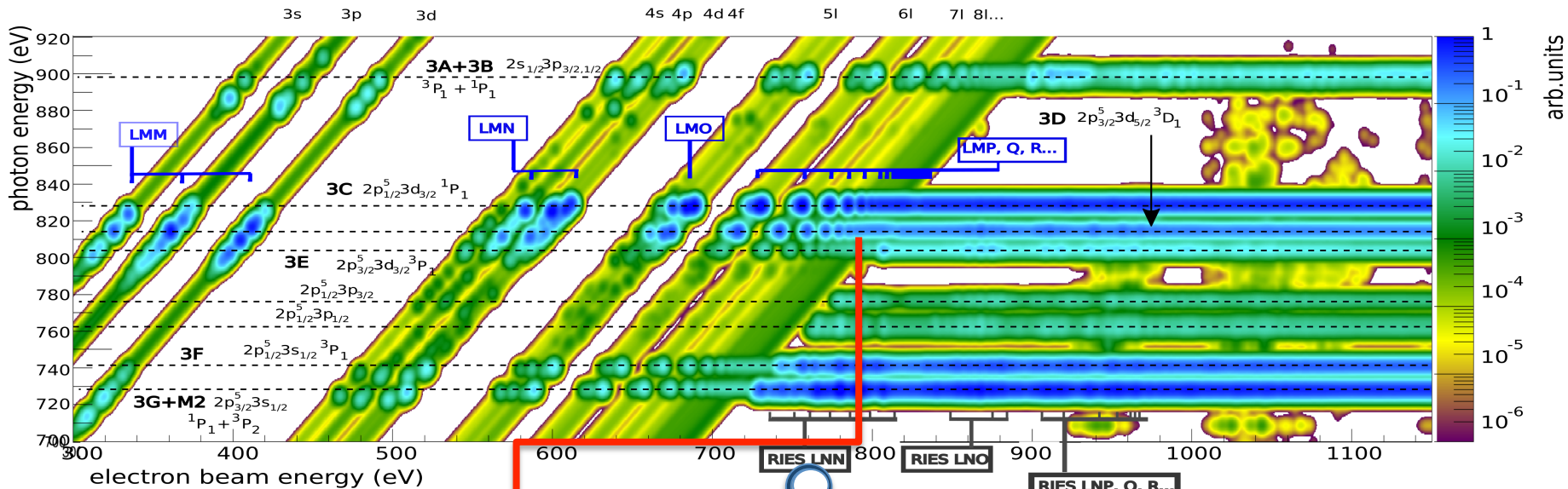
Atomic processes in Fe XVII



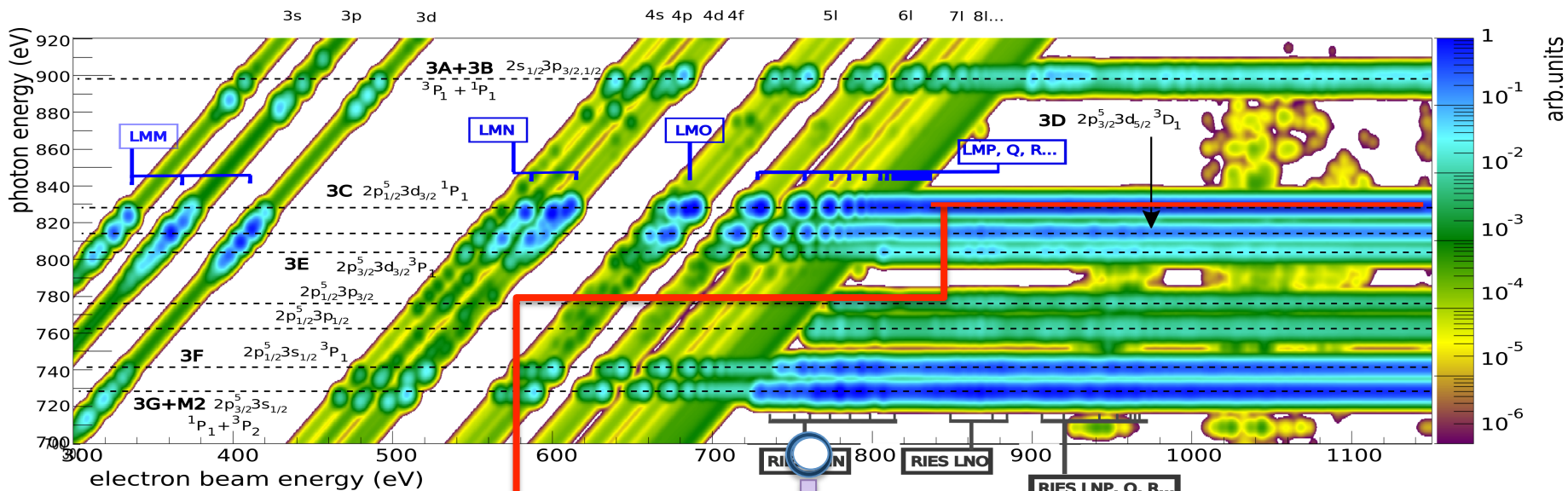
Dielectronic recombination (DR)



Atomic processes in Fe XVII

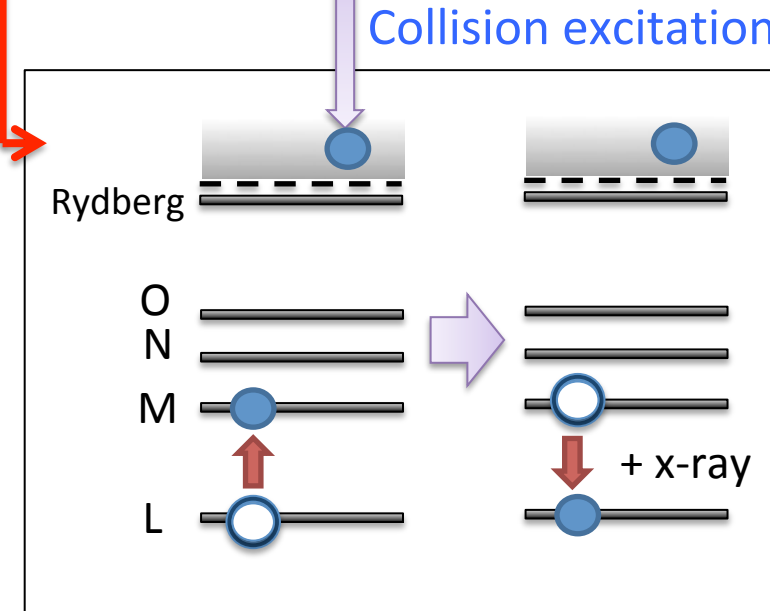


Atomic processes in Fe XVII

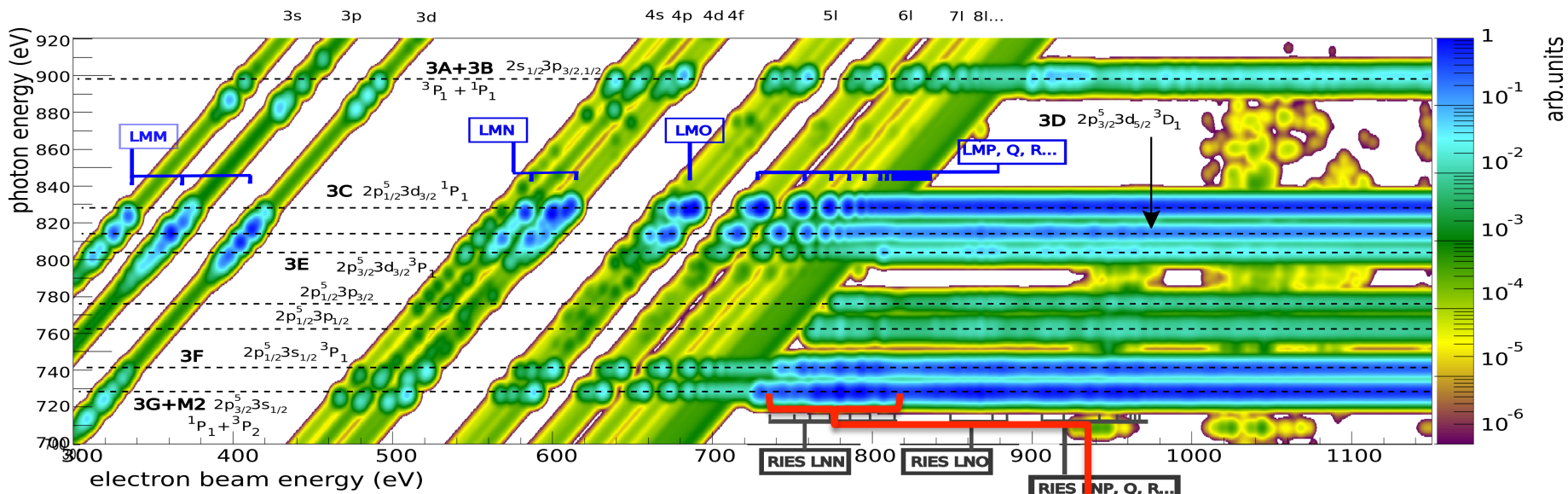


Goal of this work

- Investigate how the inclusion of the spectator electron after DR converge towards the 3C/3D CE



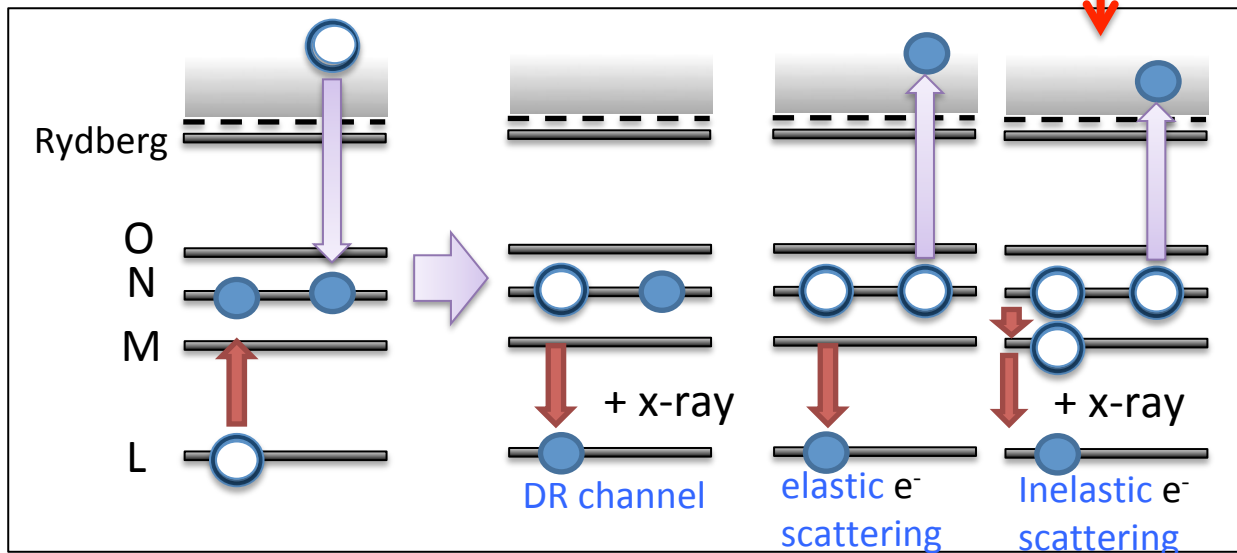
Atomic processes in Fe XVII



Dielectronic capture

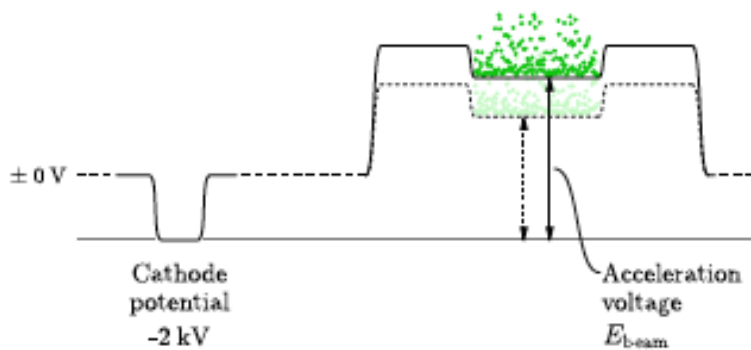
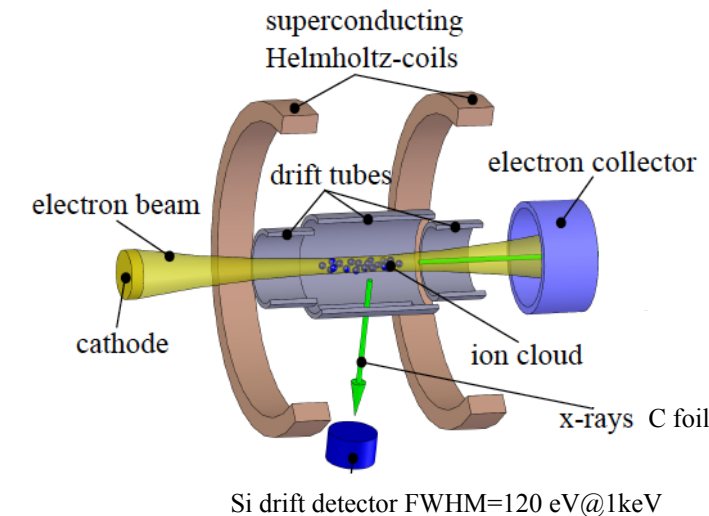
Goal of this work

- Provide data for the 3F+3G+M2 lines



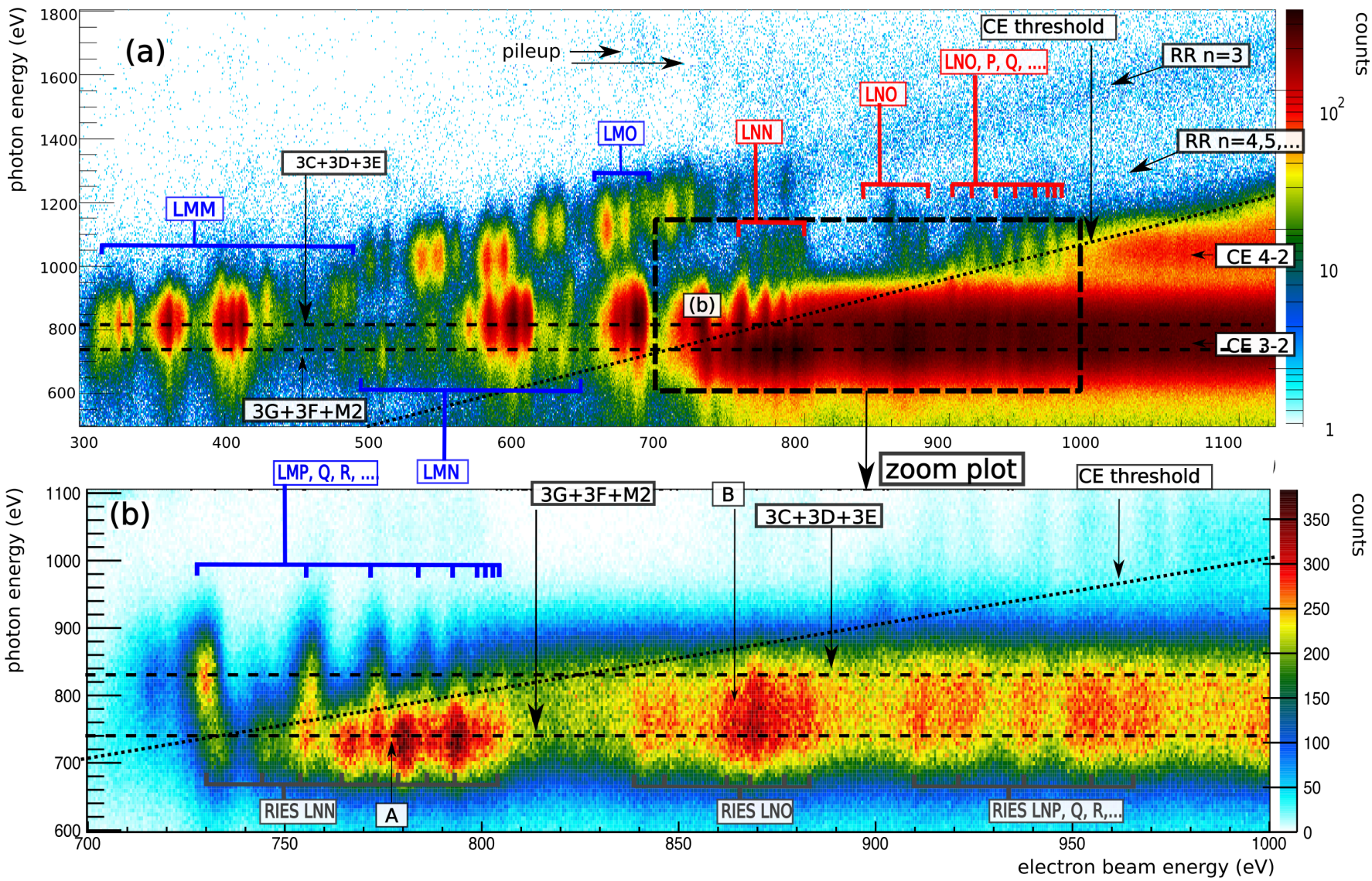
Experimental setup: electron beam ion trap

- FLASH-EBIT @Heidelberg



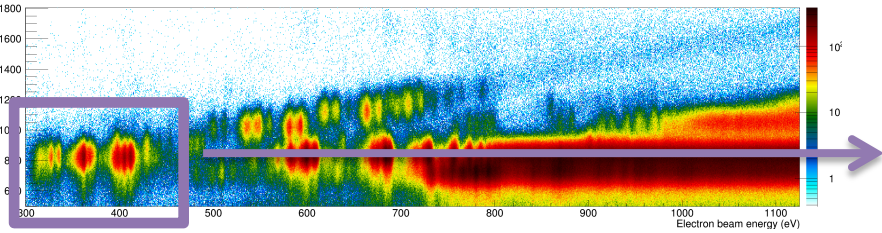
- Hot plasma with a **monoenergetic** electron beam
 - Scan setup
 - Electron density current constant
$$n_e \propto I_e / \sqrt{E}$$
 - Evaporative cooling for a electron energy resolution of **5 eV@900eV**
-
- A graph showing the voltage V versus time. The voltage is held at 0 V for 0.5s, then drops to -250 eV for 40ms, followed by a 40ms pulse at 1 kV. The graph indicates two ionization levels: Fe XVIII ioniz. @ 1.26 keV (green dashed line) and Fe XVII ioniz. @ 0.47 keV (red dashed line).

Measurement example

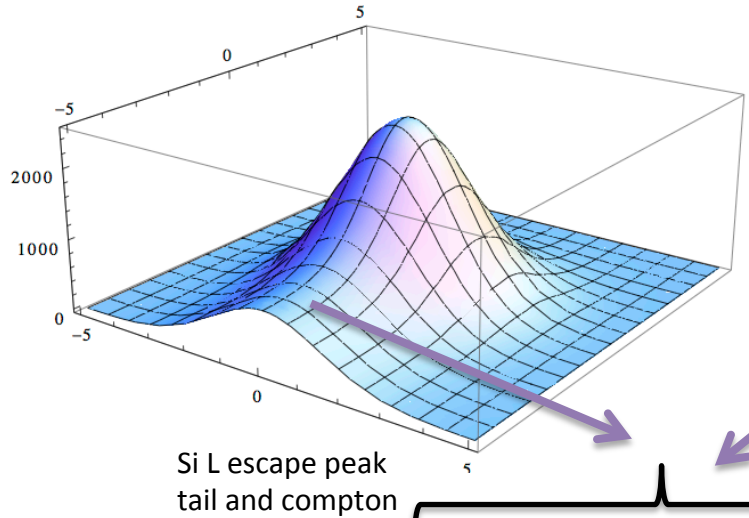


Data analyses

- 2D fit with detector response function
- Main LMM resonance used

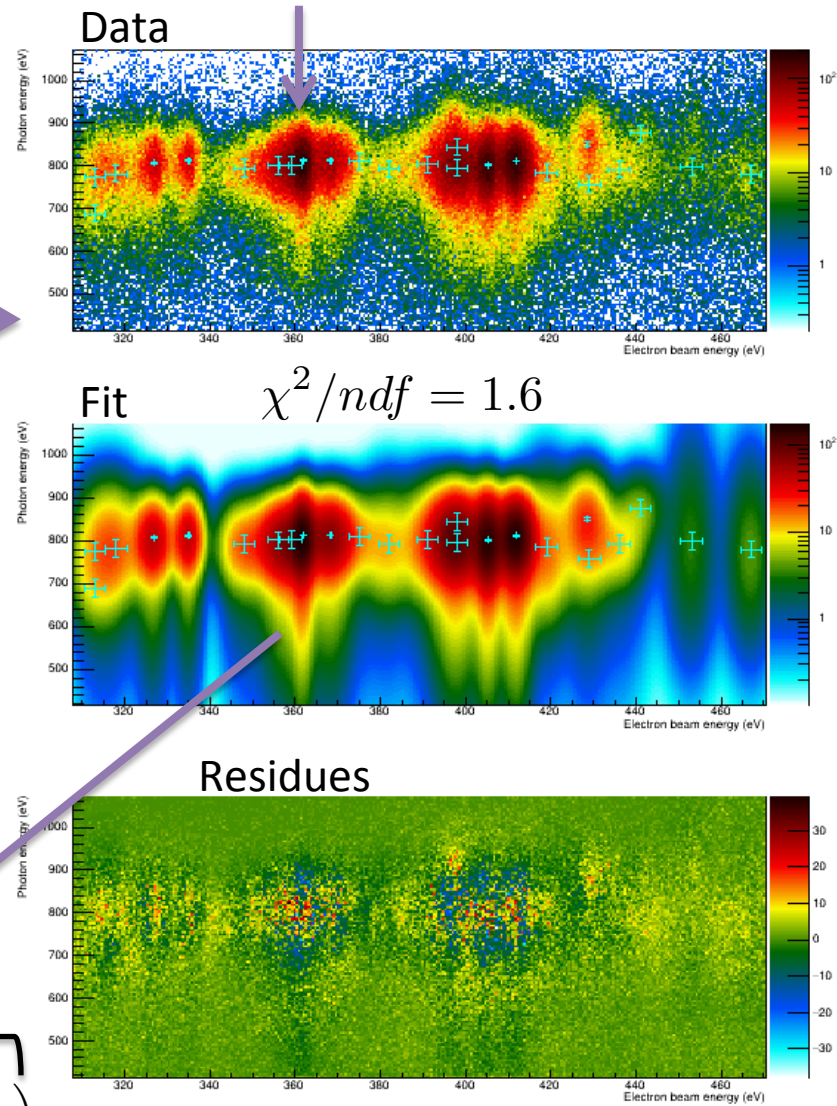


LI Zhe, et al, Nuclear Science and Techniques **24** (2013) 060206



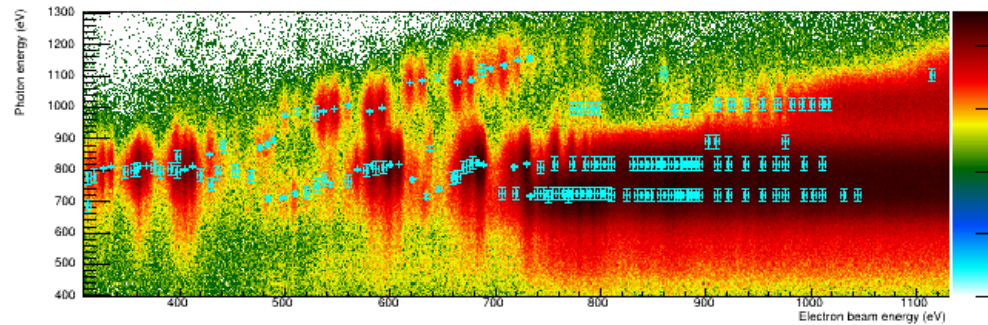
Si L escape peak tail and compton

$$f(x, y) = C_1 e^{-\frac{(x-x_0)^2}{2\sigma_x^2}} \left(C_2 e^{-\frac{(y-y_0)^2}{2\sigma_y^2}} + C_3 e^{\frac{y-y_0}{\sigma_y'}} \operatorname{Erfc} \left(\frac{y-y_0}{C_4 \sigma_y} + \frac{\sigma_y}{C_4 \sigma_y'} \right) \right)$$

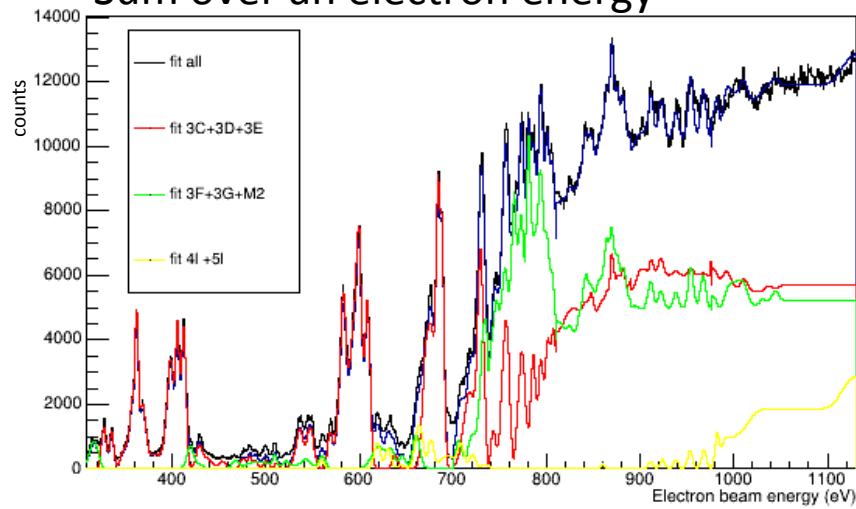


Data analyses

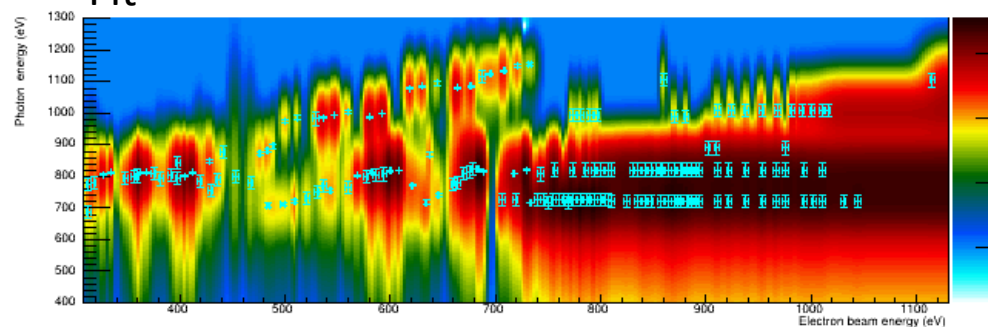
Data



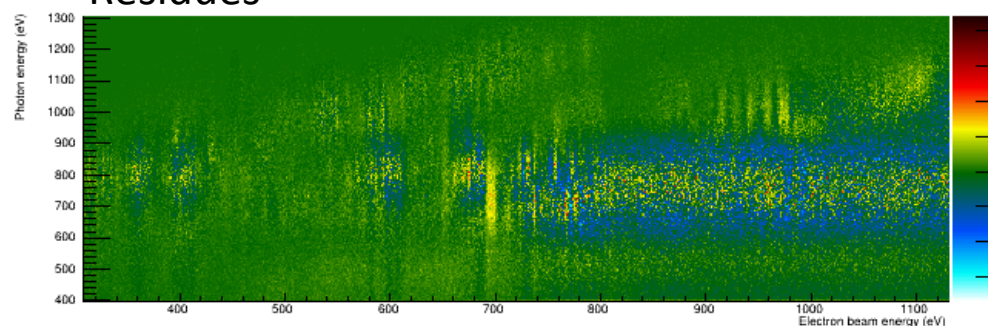
Sum over an electron energy



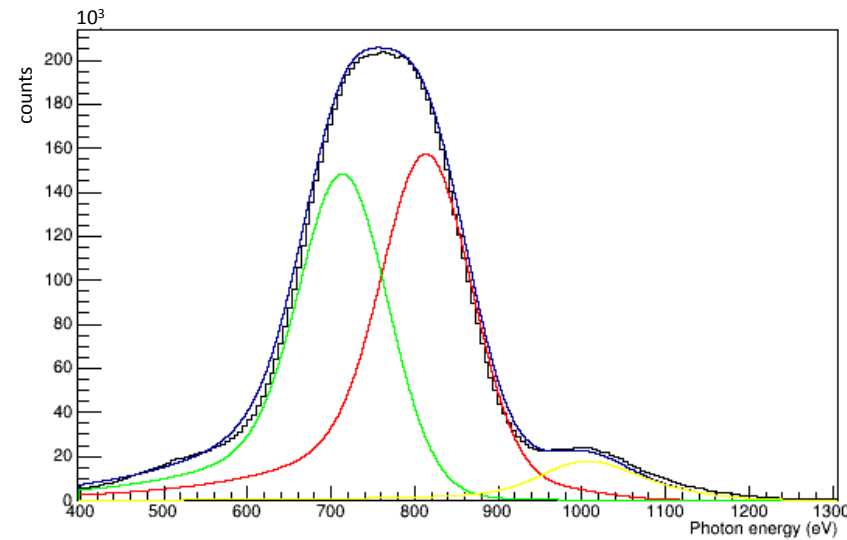
Fit



Residues



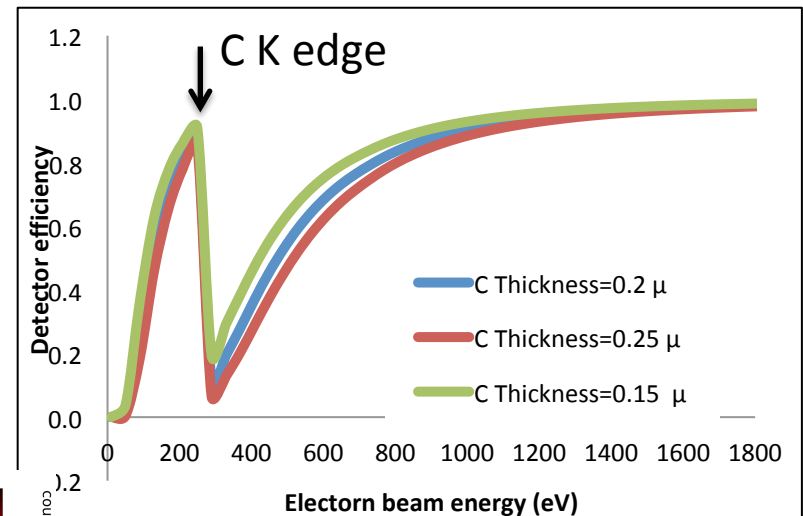
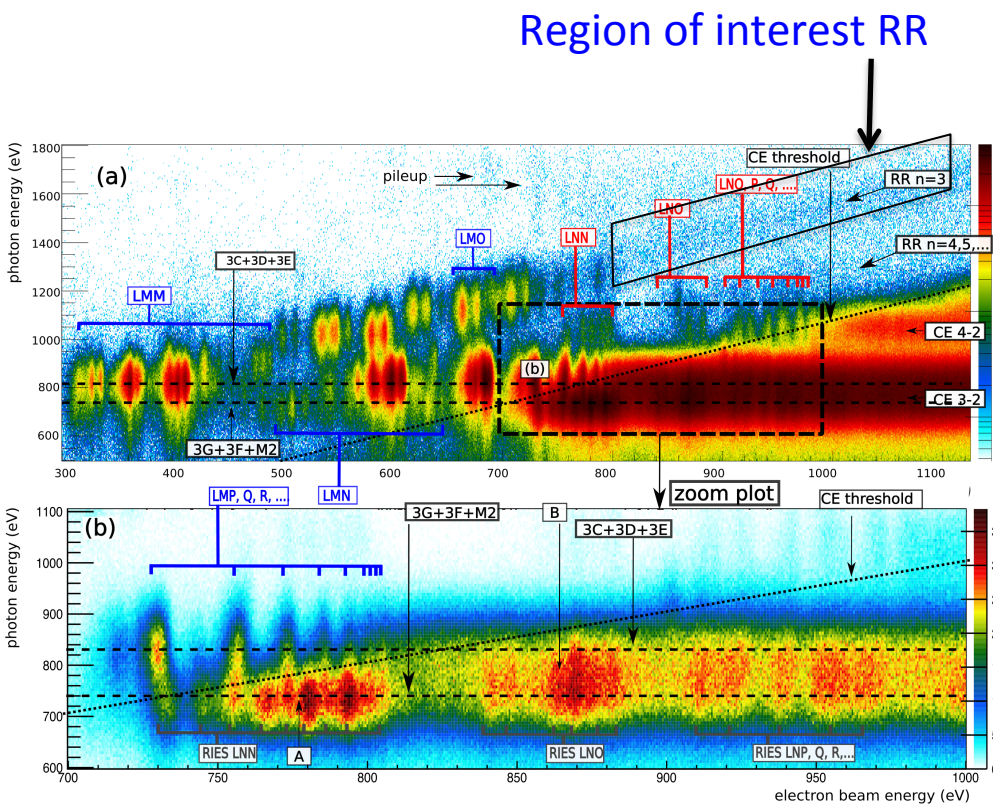
Sum for a photon energy



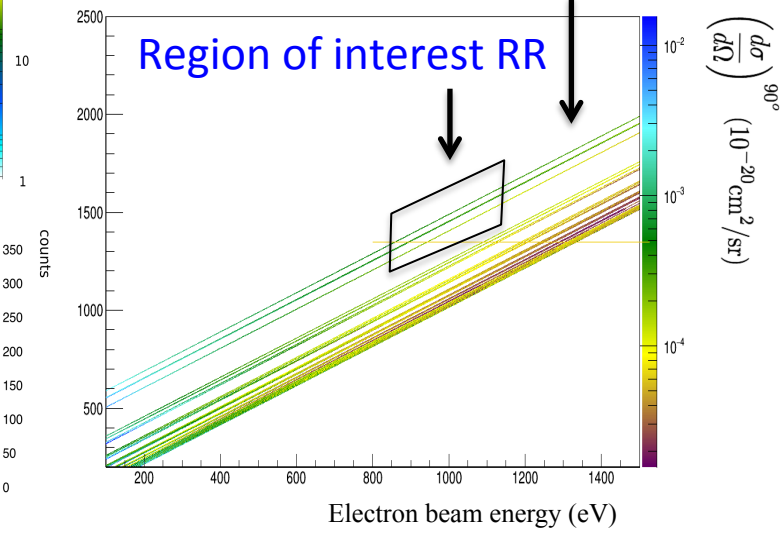
Cross section calibration based on RR

- RR cross sections calculated with 5% error
- Similar method of

G. V. Brown, et al PRL, 96, 253201 (2006)

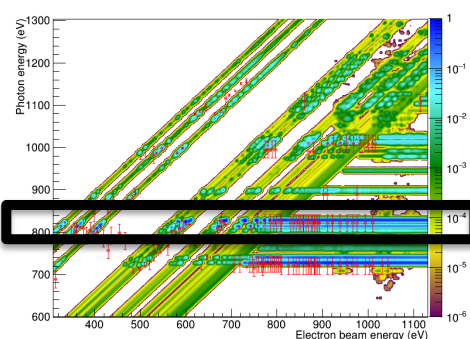
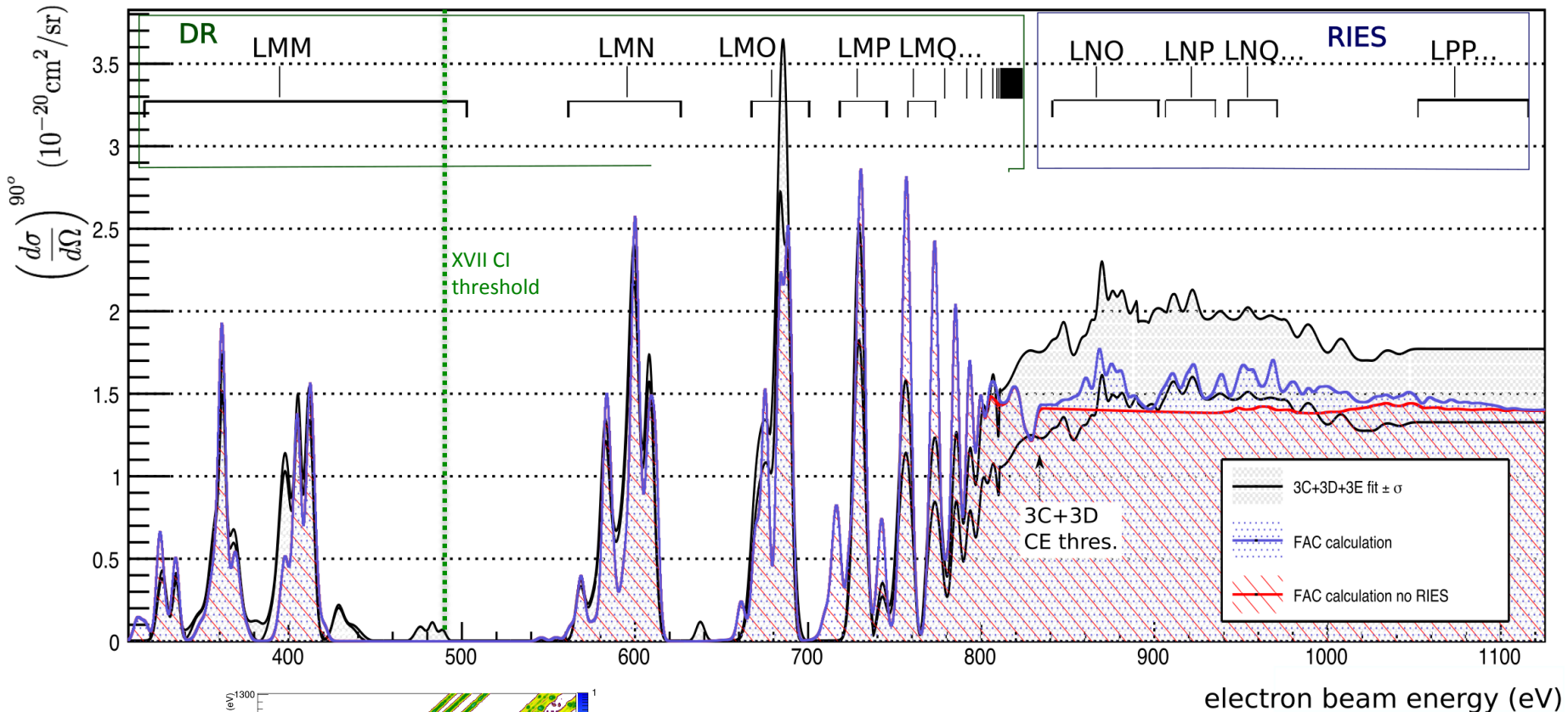


E. Saloman et al., At. Data Nucl. Data Tables 38, 1 (1988)



Results for 3C+3D+3E

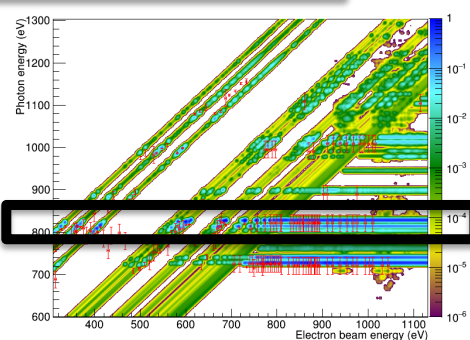
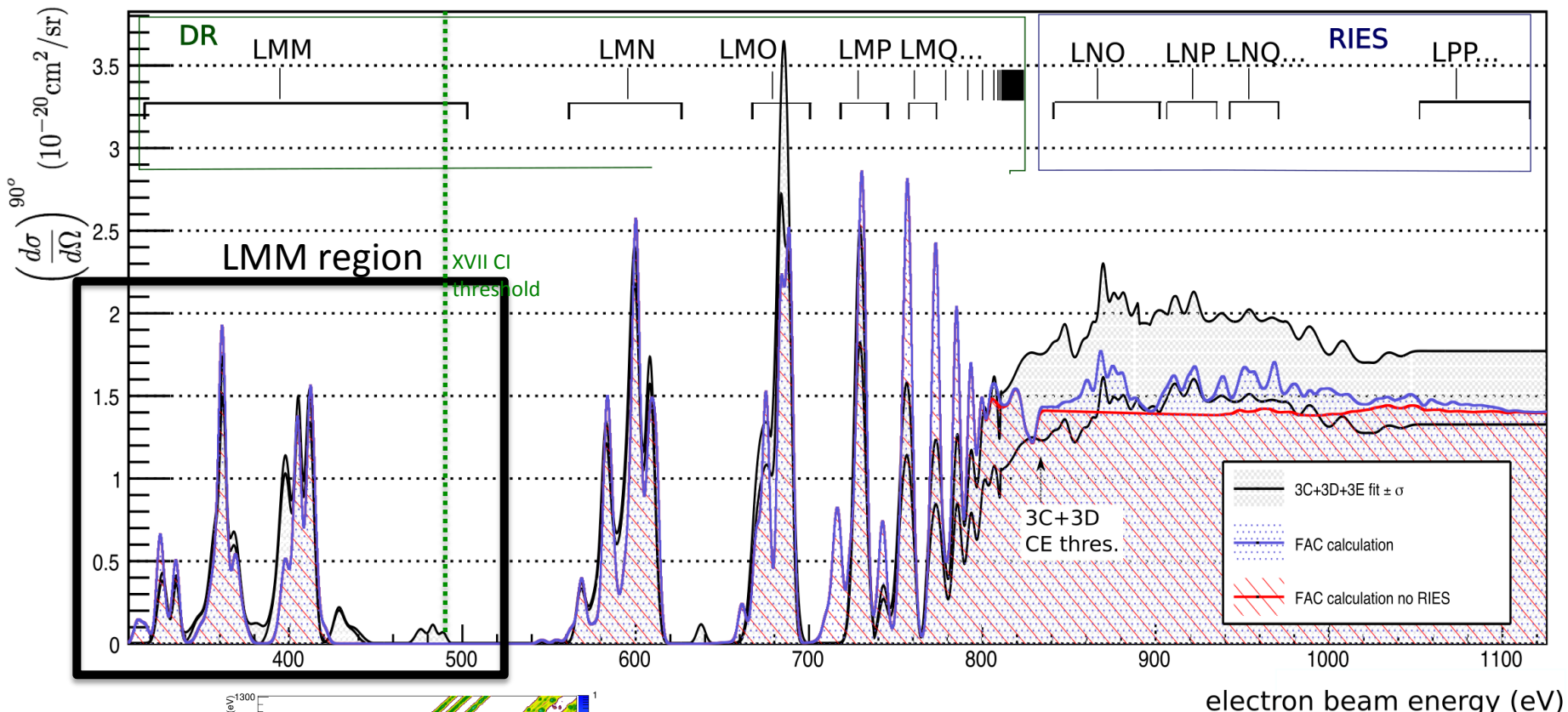
- Region of interest of 3C+3D+3E for the entire scan



FAC-Flexible atomic code

Results for 3C+3D+3E

- Region of interest of 3C+3D+3E for the entire scan

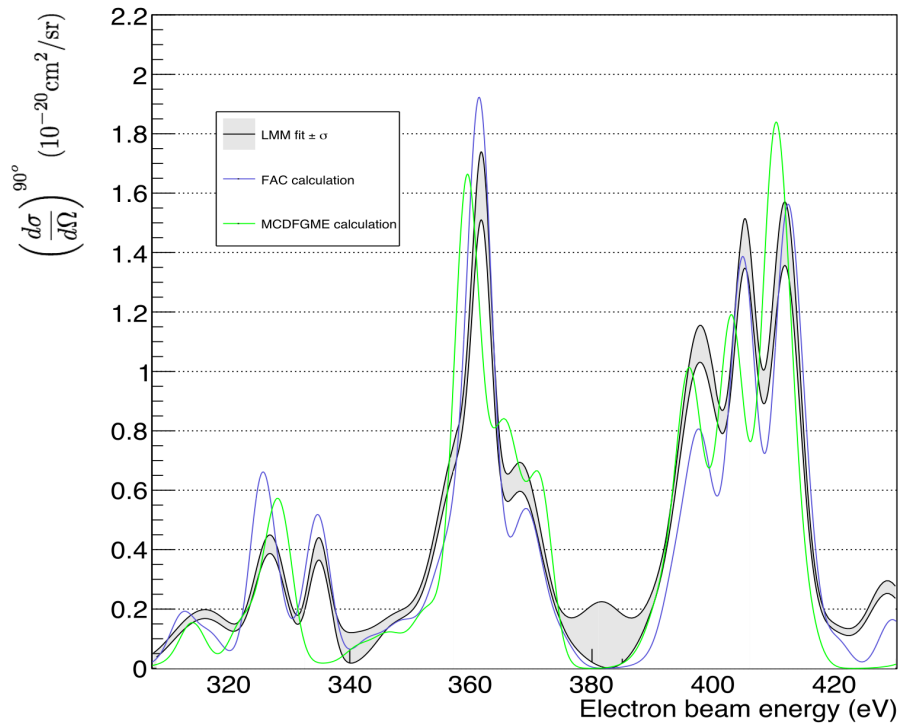


3C+3D+3E

FAC-Flexible atomic code

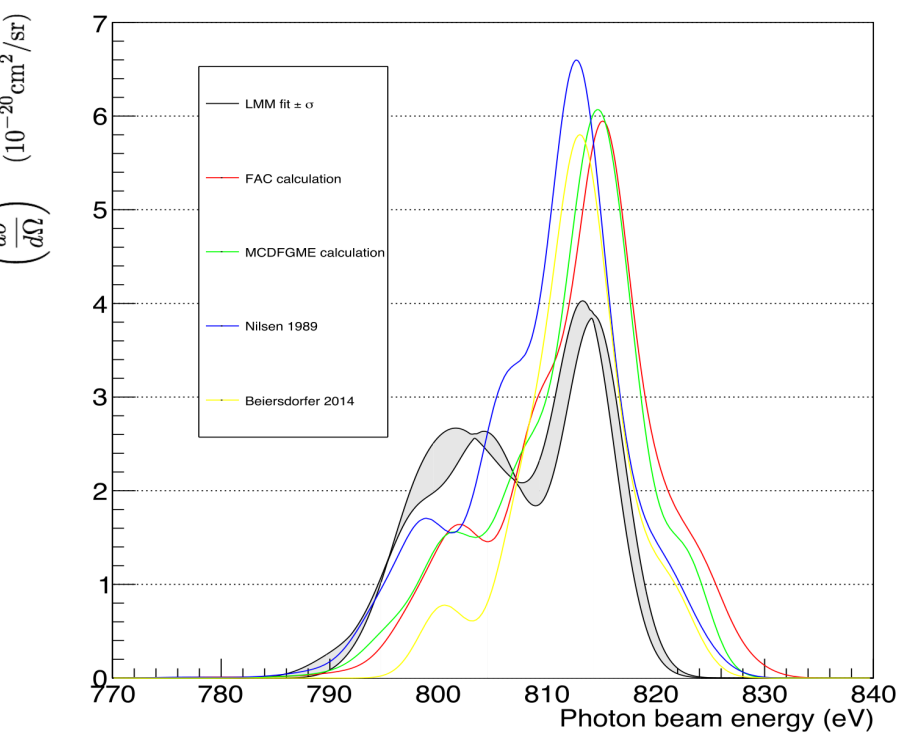
Results 3C+3D+3E LMM region

Sum over photon energy



- FAC-Flexible atomic code
- Multiconfiguration Dirac-Fock (MCDFGME) code of P. Indelicato and J.-P. Desclaux

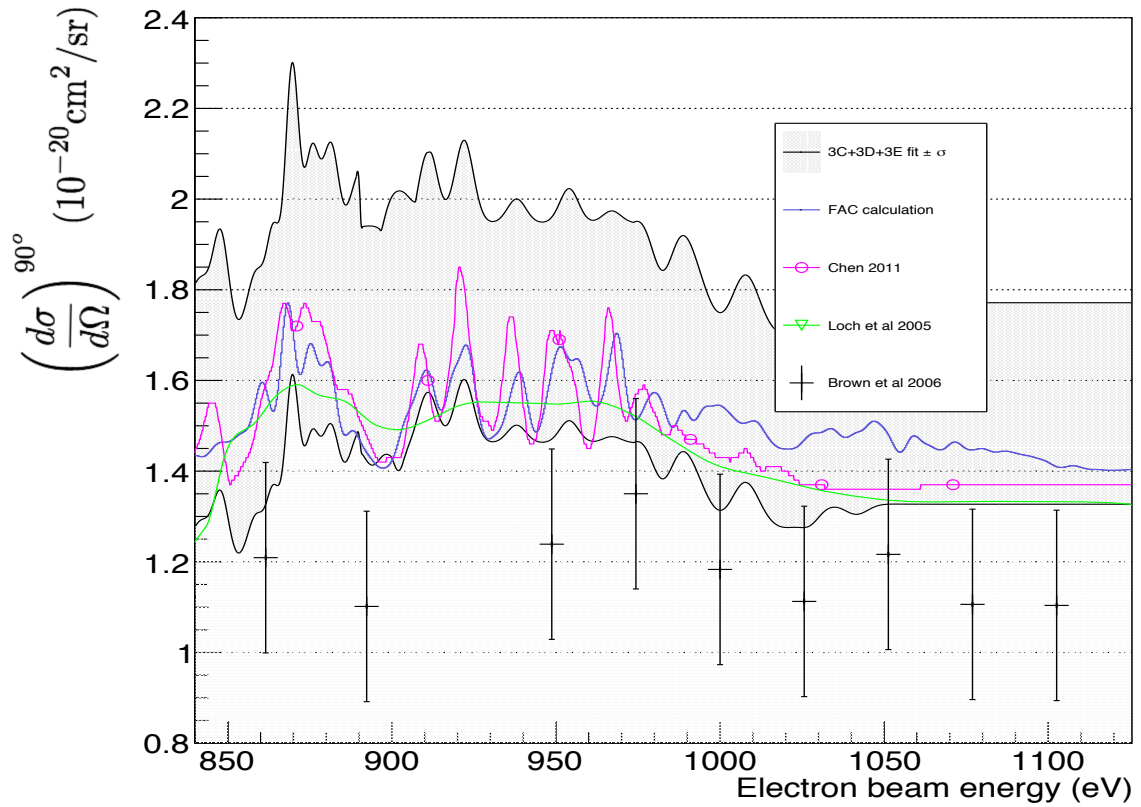
Sum over electron energy **Preliminary**



- J. Nilsen, Atomic Data and Nuclear Data Tables, 41, 131, (1989), multiconfiguration Dirac-Fock
- P. Beiersdorfer *et al*, ApJ, 793, 99, (2014) relativistic multi-reference Møller–Plesset perturbation theory

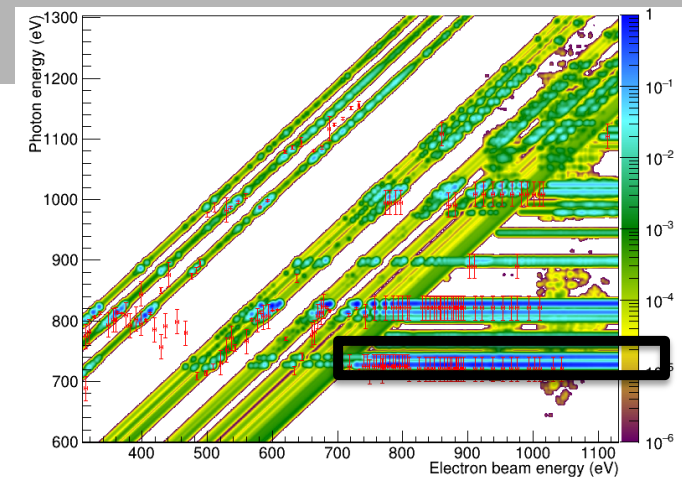
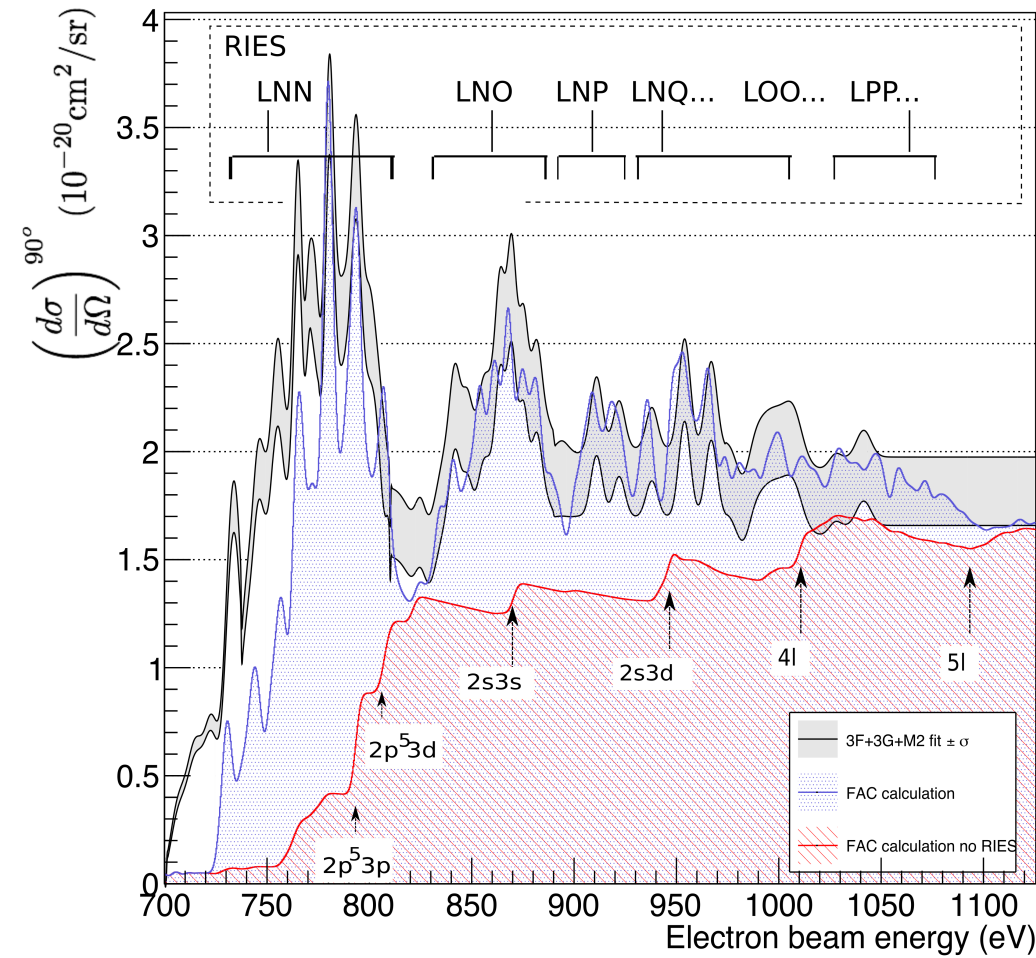
Results 3C+3D+3E CE region

- G. X. Chen and A. K. Pradhan, PRL, 89, 013202 (2002) 30 eV broadening ; G. X. Chen PRA, 84, 012705 (2011) 5 eV broadening. Couple-cluster Breit-Pauli/Dirac R-matrix
- S. D. Loch, JPB 39, 85 (2005), 30 eV broadening, relativistic R-matrix calculation
- G. Brown *et al*, PRL, 96, 253201 (2006). Experimental calibrated with RR (E. Saloman et al., At. Data Nucl. Data Tables 38, 1 (1988).)

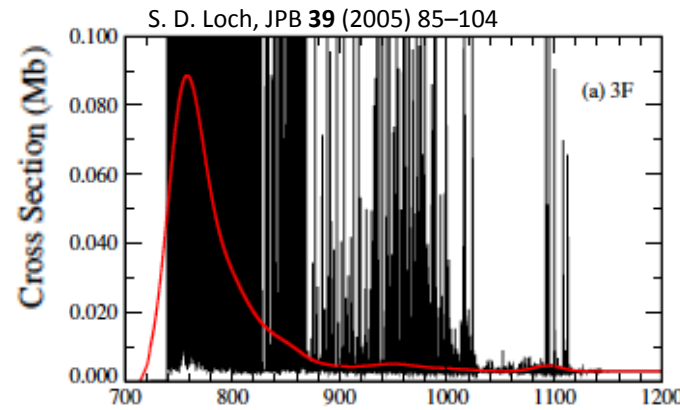


Results 3F+3G+M2

- Region of interest of 3F+3G+M2



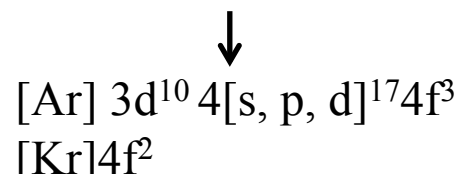
- Complex cascade contribution from forbidden transitions into ground state
- Pronounced contribution of RIES



Electron recombination in tungsten

- Energy region of MNN

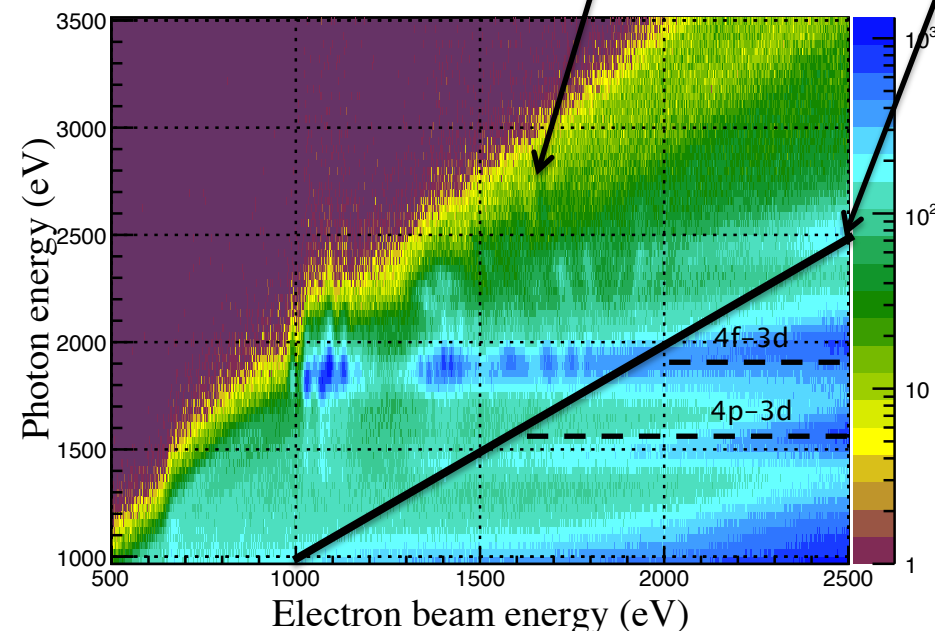
MNN channel in Ag-like W



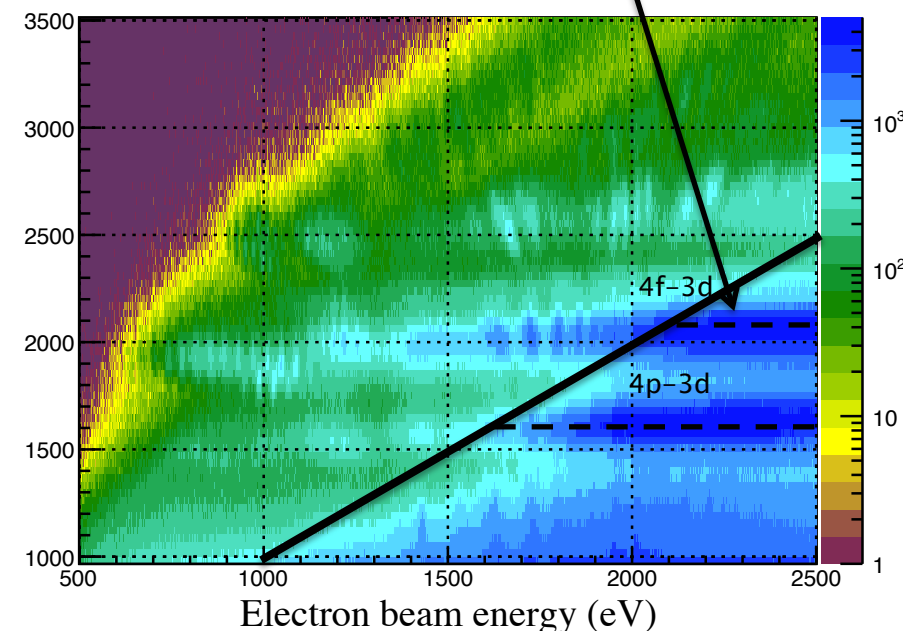
CE threshold

RIES contribution

(a) scan upwards



(b) scan downwards



Summary of the goals

- ✗ Investigate how the inclusion of the **spectator electron after DR** converge towards the 3C/3D CE
 - ☐ LMM structure predicated over the electron energy. Photon energies require further verification
 - ✓ No conclusion can be obtain for the **3C/3D conundrum in the CE region** within the error bars
 - ✓ Pronounced discrepancy on **DR** after $n=4$
 - ✓ Synthetic maxwellian emission based on experimental centroids to be compared with satellite-mission spectra
- ✓ Provide data for the 3F+3G+M2 lines
 - ✓ Agreement with theory within error bars
 - ✓ RIES mechanism and the complex cascades are predicated

Ionization cross sections

Scattering Cross Sections

Relativistic Version of Binary-encounter Model

PHYSICAL REVIEW A, VOLUME 62, 052710

Extension of the binary-encounter-dipole model to relativistic incident electrons

Yong-Ki Kim

National Institute of Standards and Technology, Gaithersburg, Maryland 20899-8423

José Paulo Santos

Departamento de Física, Faculdade de Ciências e Tecnologia, Universidade Nova de Lisboa, Monte de Caparica, 2825-114 Caparica, Portugal

and Centro de Física Atómica da Universidade de Lisboa, Avenida Professor Gama Pinto 2, 1649-003 Lisboa, Portugal

Fernando Parente

Departamento Física da Universidade de Lisboa and Centro de Física Atómica da Universidade de Lisboa, Avenida Professor Gama Pinto 2, 1649-003 Lisboa, Portugal

(Received 18 May 2000; published 13 October 2000)

- $T \longrightarrow$ Kinetic energy of the incident electron
- $W \longrightarrow$ Kinetic energy of the ejected electron
- $a_0 \longrightarrow$ Bohr's radius
- $R \longrightarrow$ Rydberg's constant
- $T-W \longrightarrow$ Kinetic energy of the scattered electron

$$\sigma_{RBEB}(t) = \frac{4\pi a_0^2 \alpha^4 N}{(\beta_t^2 + \beta_u^2 + \beta_b^2) 2b'} \left[\frac{1}{2} \left[\ln\left(\frac{\beta_t^2}{1-\beta_t^2}\right) - \beta_t^2 - \ln(2b') \right] \left(1 - \frac{1}{t^2}\right) \right.$$

$$\left. + 1 - \frac{1}{t} - \frac{\ln t}{t+1} \frac{1+2t'}{(1+t'/2)^2} + \frac{b'^2}{(1+t'/2)^2} \frac{t-1}{2} \right]$$

$$\begin{aligned} t' &= T/mc^2 & \beta_t &= v_t/c \\ b' &= B/mc^2 & \beta_b &= v_b/c \\ u' &= U/mc^2 & \beta_u &= v_u/c \end{aligned}$$

$$\beta_t^2 = 1 - \frac{1}{(1+t')^2}$$

$$\beta_b^2 = 1 - \frac{1}{(1+b')^2}$$

$$\beta_u^2 = 1 - \frac{1}{(1+u')^2}$$

Total Ionization of Highly Charged Ions

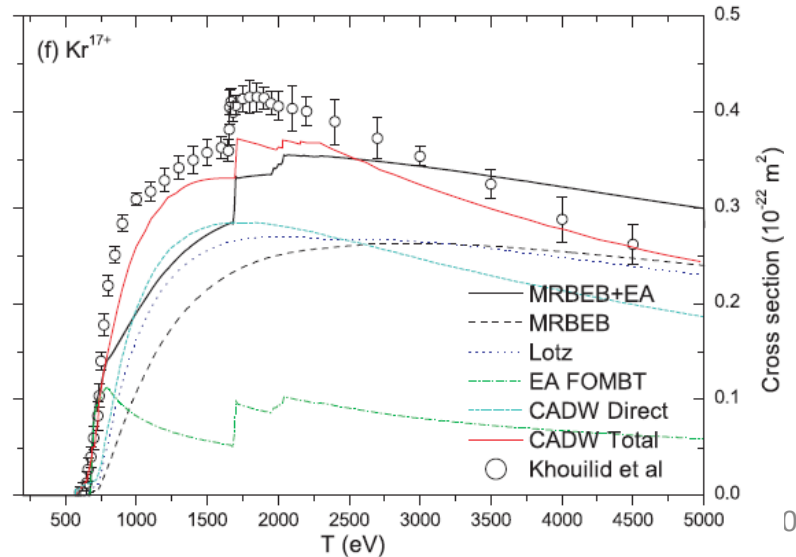
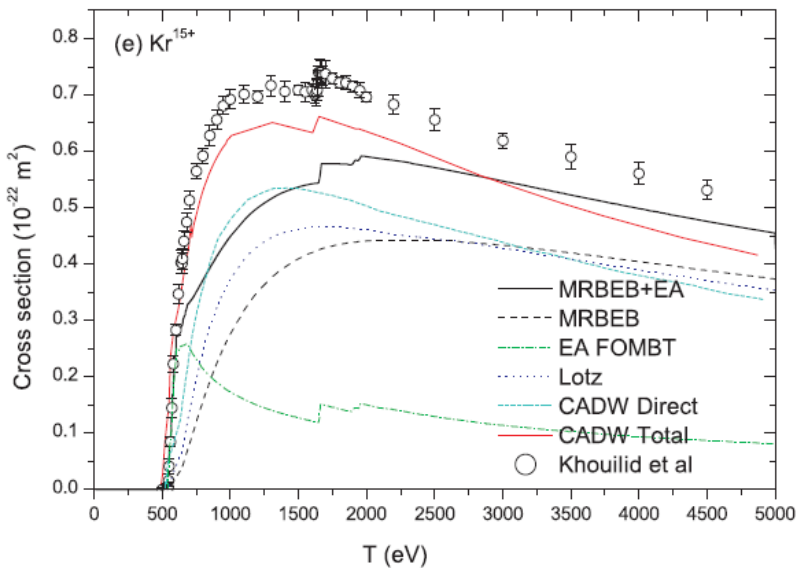
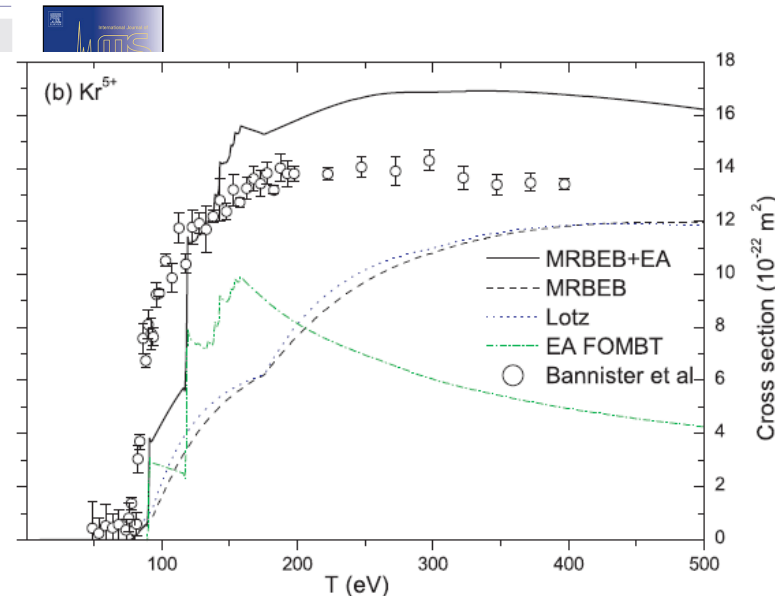
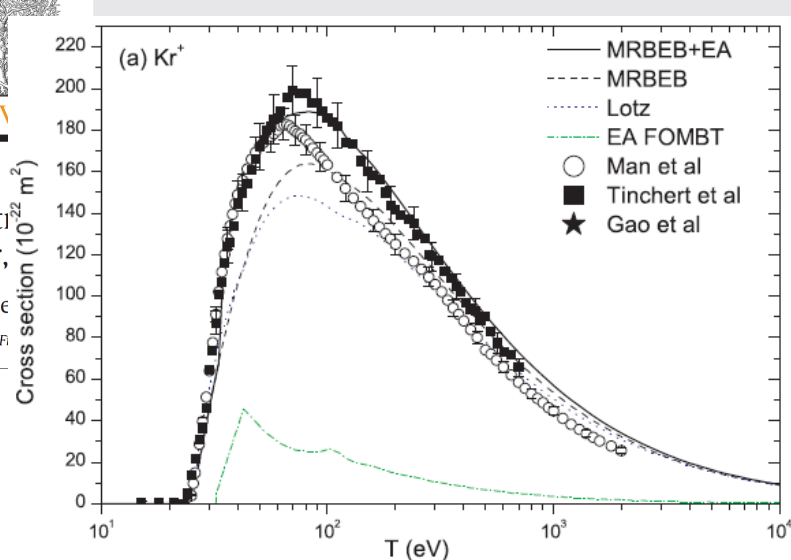
Modified Binary Encounter Bethe Model

International Journal of Mass Spectrometry 348 (2013) 1–8



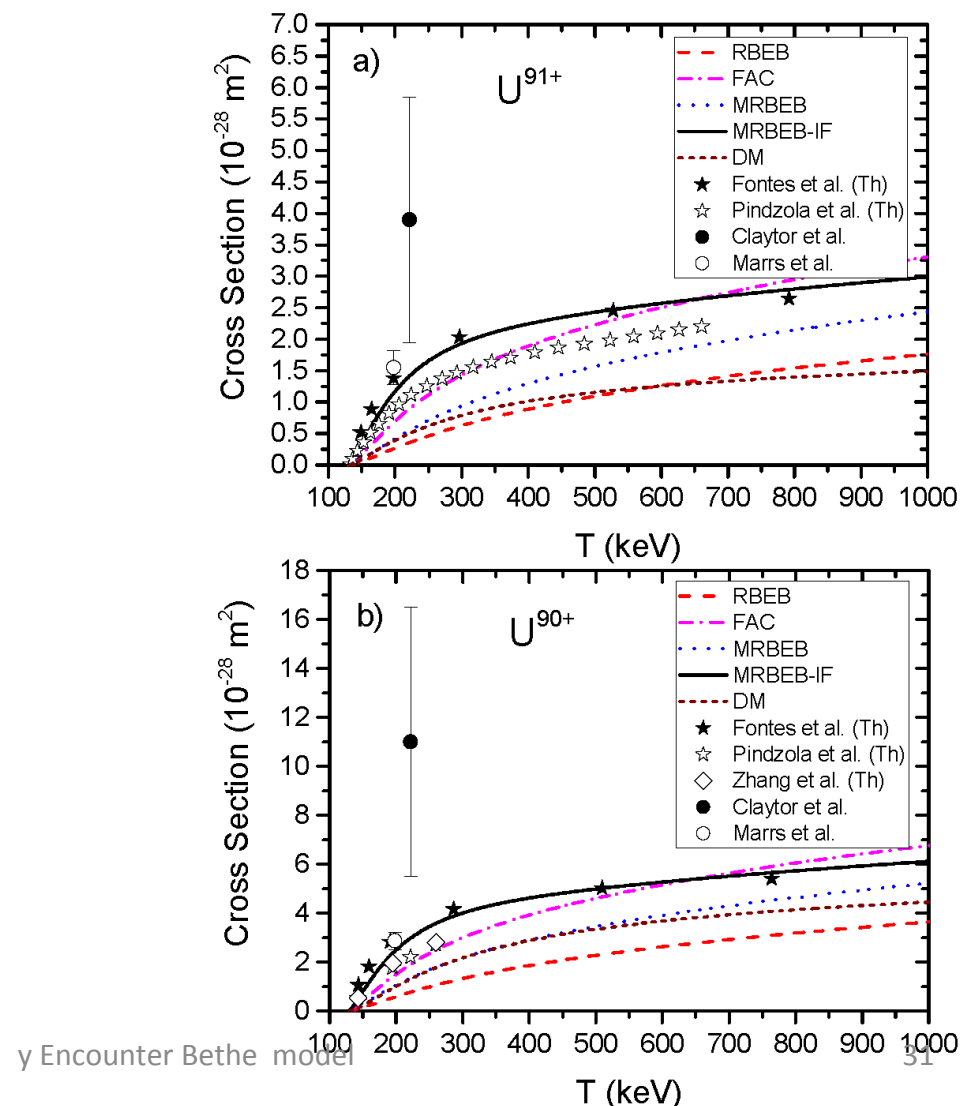
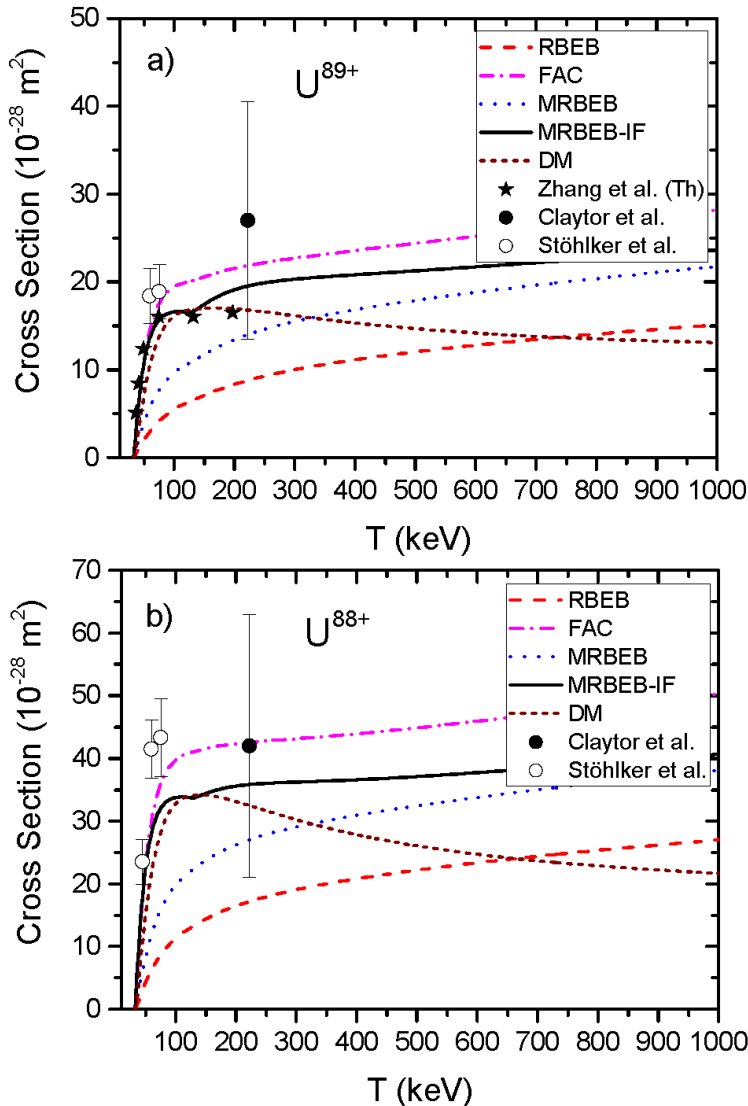
Electr.
of Kr,
M. Gue
Centro de F

Contents lists available at SciVerse ScienceDirect



Total Ionization of Highly Charged Ions

Electron impact ionization cross sections for

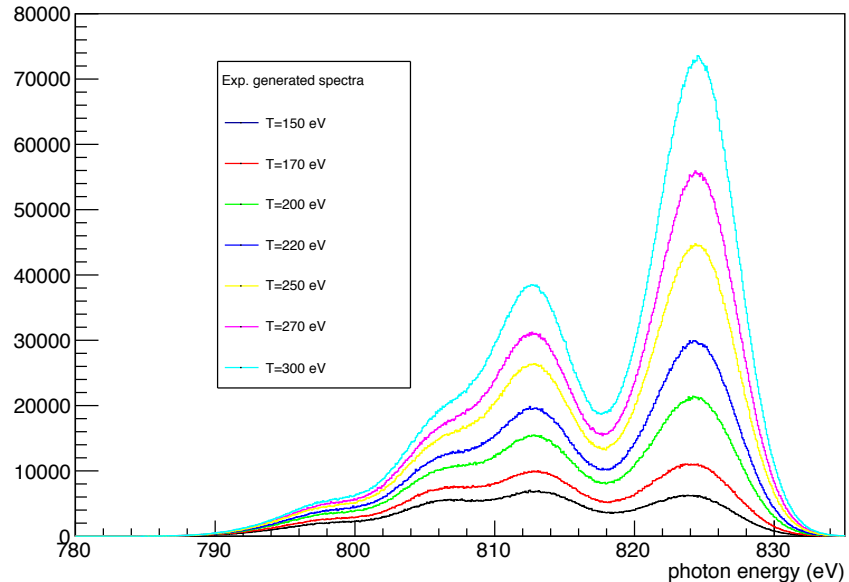
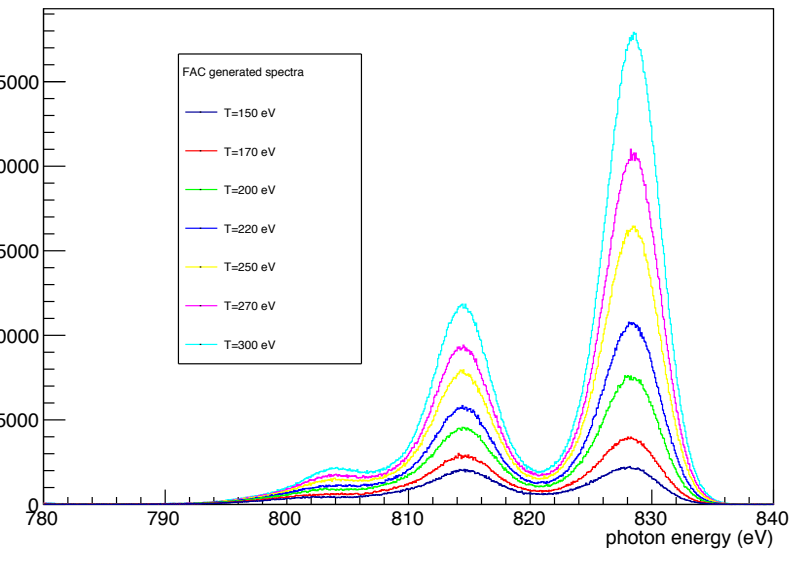
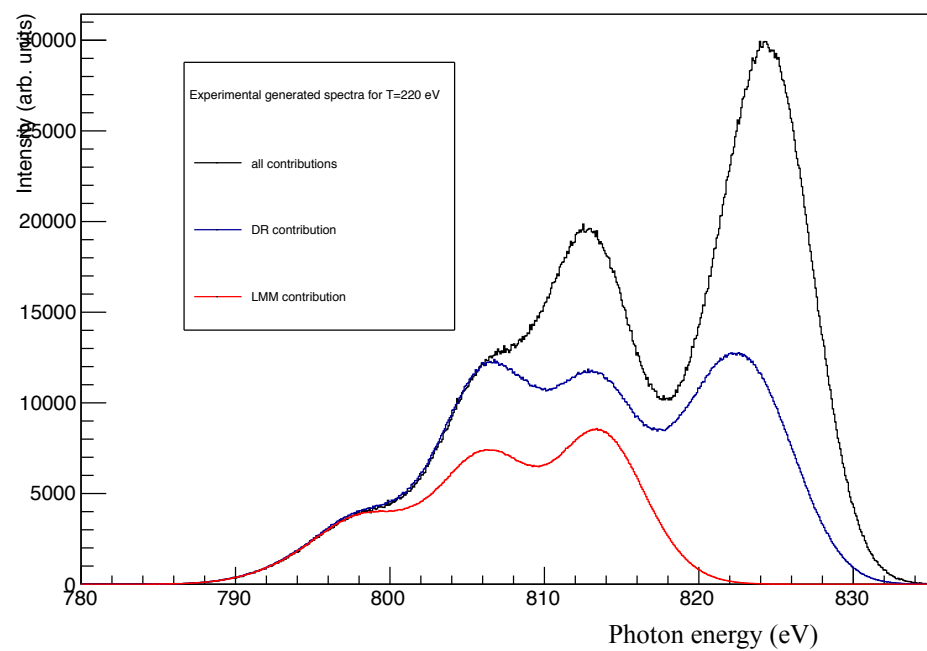
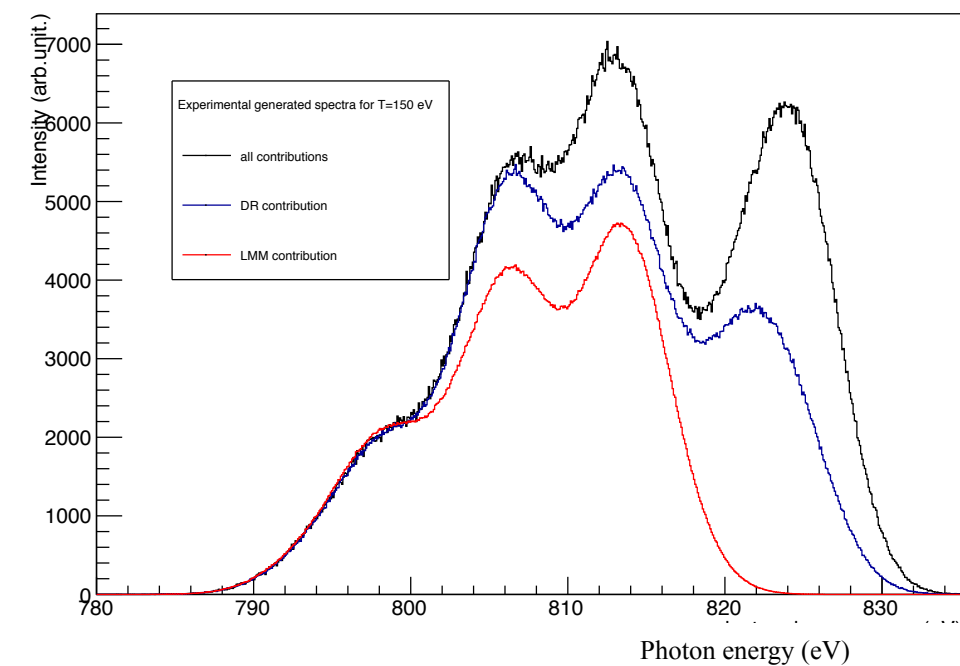


Summary of the goals

- ✓ Provided cross sections based in the MRBEB
 - ✓ Several ionization states of Kr
 - ✓ H- and He-like U
- Test the MBEB/MRBEB expression for the ionization of ions in several charge states
- Include results of this expression in a user-friendly website

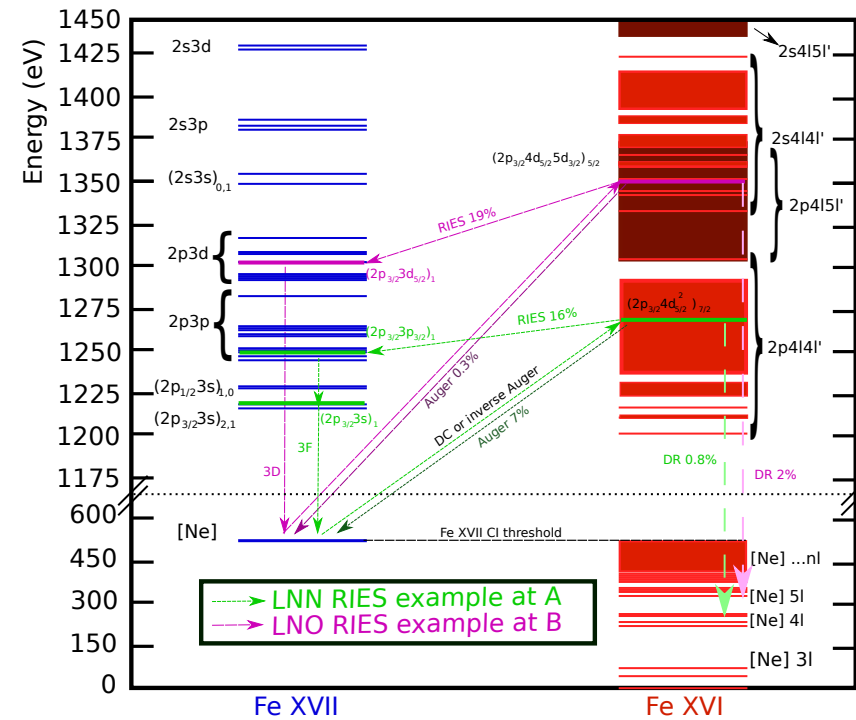
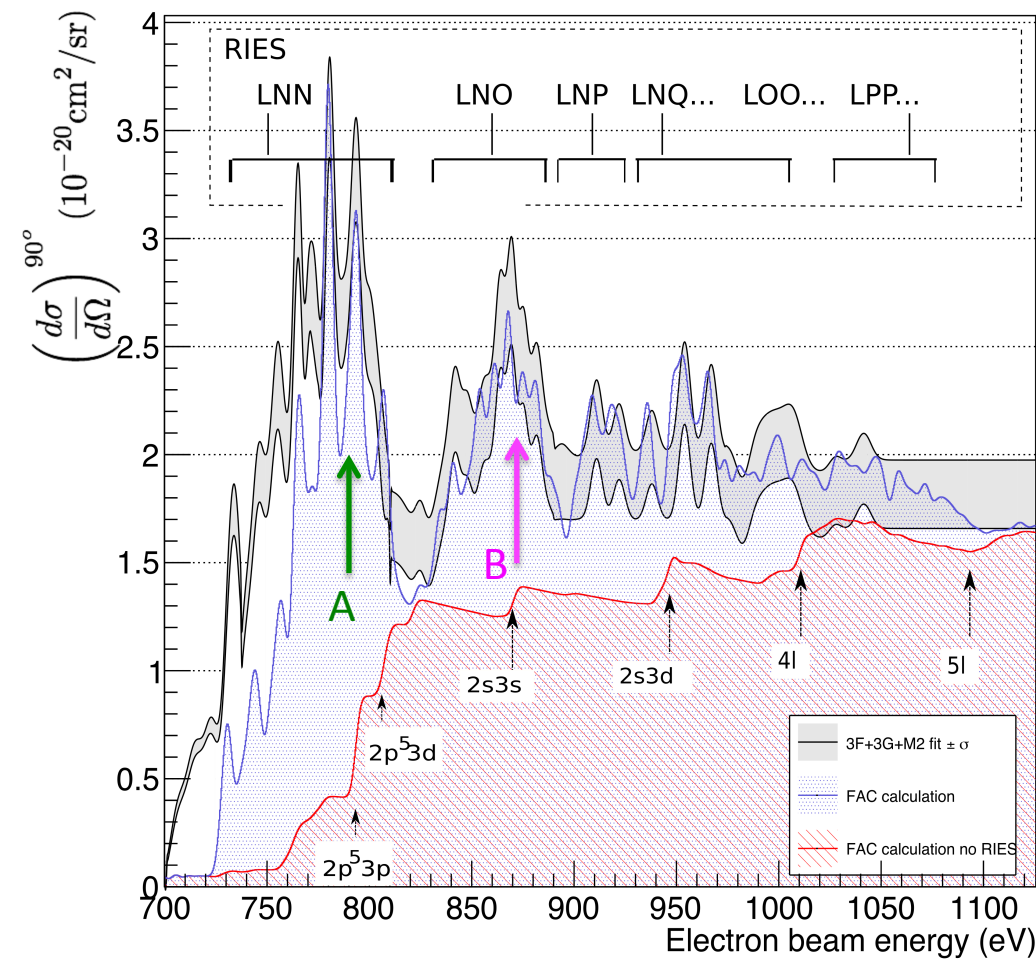
Thanks for your attention

Results 3C+3D+3E CE region Maxwell distribution



Results 3F+3G+M2

- Region of interest of 3F+3G+M2



Fe XVII purity during scan

